Frontiers in Heat and Mass Transfer

Tech Science Press

DOI: 10.32604/fhmt.2025.059710

REVIEW

Conveyor Belt Crop Dryer Modelling: A Comprehensive Review

Gehad Azmy, Mohamed El-Morsi and Omar Abdelaziz*

Department of Mechanical Engineering, The American University in Cairo (AUC), New Cairo, 11835, Egypt

*Corresponding Author: Omar Abdelaziz. Email: omar_abdelaziz@aucegypt.edu

Received: 15 October 2024 Accepted: 19 December 2024 Published: 26 February 2025

ABSTRACT

This review paper presents an in-depth investigation of the modeling techniques used to study conveyor belt dryers. These techniques are classified into four categories: theoretical modeling, computational fluid dynamics (CFD), empirical, and performance under different control strategies. Within the theoretical and CFD categories, the models are further classified as transient and steady state, as well as one-dimensional, two-dimensional, and three-dimensional. The empirical approach involves conducting experimental studies to collect moisture ratio data during the drying process and comparing it with empirical models. The methods of control are divided into classical and advanced controllers, with classical controllers including proportional-integral (PI), proportional-integral-derivative (PID), and quantitative feedback theory (QFT) controllers. Advanced controllers consist of artificial intelligence-based controllers, such as artificial neural networks (ANN), adaptive neuro-fuzzy inference systems (ANFIS), nonlinear autoregressive exogenous (NARX) models, model predictive control (MPC), and soft sensors. This review elucidated the methodologies and software employed for each modeling technique, as well as their prospective utility in industrial contexts. The utilization of theoretical and CFD methodologies is advantageous in forecasting the dynamics of complex systems. Conversely, empirical techniques serve the purpose of validating theoretical models and procuring data to facilitate model refinement. Controllers play a crucial role in the optimization of the drying process and the attainment of desired outputs.

KEYWORDS

Conveyor belt drying; belt drying; convective drying

Nomenclature

a_W	Water activity of air stream leaving the product	
$A_{product}$	Specific surface area of product	m^2
B_I	Width of the product bed	m
c	Specific heat capacity	J/kg.K
D	Diffusion coefficient of the moisture vapor in the air	m^2/s
D_C	Capillary diffusivity of water in air	m^2/s
D_{cons}	Drying constant	
D_g	Water diffusion coefficient in the gas phase	m^2/s
DP	Drying potential	kJ/kg_{vapor}

DP_{th}	Thermodynamically drying potential	kJ/kg$_{vapor}$
Fm_P	Evaporation mass flux density in one pellet	kg/m^2.s
G_{air}	Mass velocity of drying air	kg/m^2.s
h_m	Heat Transfer coefficient	W/m^2.K
H_I	Height of the product bed	m
H_R	Relative Humidity of air	%
k_{m}	Mass Transfer coefficient	m/s
K	Thermal conductivity	W/m^2.K
L_{Belt}	Length of the belt	m
$\dot{m}_{air}$	Air mass flow rate	kg/s
MR	Moisture ratio	
p_{wvs}	Partial pressure of water vapor on–surface of moist material	Pa
Pr	Prandtl number	
r	Thermal Energy	kJ
R	Outside surface moisture index	
Re	Reynolds Number	
R_{wv}	Gas constant of water vapour	J/kg.K
t	Time	s
T_0	Absolute zero	°C
T	Residence time	s
$T_{product}$	Product temperature	°C
U_{air}	Air velocity	m/s
U_{Belt}	Velocity of the belt	m/s
ν	Kinematic viscosity	m^2/s
X	Moisture content of the product	kg$_{water}$/kg$_{dry\ solid}$
X_E	Equilibrium moisture content of the product	kg$_{water}$/kg$_{dry\ solid}$
X_{air}	Absolute humidity of air stream	kg$_{water}$/kg$_{dry\ solid}$
ΔT_{mL}	Logarithmic mean temperature difference	
ρ_{product}	Density of the product	kg/m^3
β	Material porosity	
μ_{air}	Viscosity of drying air	Pa.s

1 Introduction

Crop preservation through drying is a well-established method [1], reducing moisture content to inhibit microbial activity and enzymatic reactions that cause spoilage [2]. By maintaining low moisture levels, dried products can be stored at room temperature without compromising quality, leading to significant cost savings [3]. Food drying involves convection or conduction heat and mass transfer [4]. Drying techniques primarily include convective and conductive methods. Over 400 designs have been reported in the literature [4]. Convective drying, where the heating medium directly contacts the product, is the most common, accounting for over 85% of industrial drying applications. Conversely, conductive drying transfers heat indirectly, often utilizing specialized equipment to preserve heat-sensitive materials [5].

Within the broad scope of drying technologies, conveyor belt dryers have emerged as a versatile and efficient choice, especially for continuous drying processes [6]. Continuous conveyor belt dryers are particularly valued in the food industry for their ability to handle a range of products, providing high

throughput and uniform drying. By continuously moving the product through the drying chamber, conveyor belt dryers help prevent damp zones and ensure consistent quality [6].

This review specifically focuses on conveyor belt dryers used in agricultural crop drying, with a comprehensive analysis of the various modeling techniques applied to study these systems. Unlike previous review articles, which often focus on type of dryer, this work consolidates multiple modeling techniques—including theoretical models, computational fluid dynamics (CFD), and empirical approaches—to provide a holistic perspective on conveyor belt drying. The novelty of this review lies in its comparative approach, evaluating each technique's benefits, limitations, and practical applications in crop drying.

Furthermore, this paper explores control strategies that enhance the performance of conveyor belt dryers, detailing how different controllers are implemented and optimized to maintain precise drying conditions. To aid in understanding, a comparative table highlights the strengths and limitations of each modeling approach, guiding researchers in selecting the techniques that are best suited for their application requirements.

The goal of this review is to provide a valuable resource for researchers and practitioners interested in the modeling and optimization of conveyor belt dryers, contributing to advancements in agricultural drying processes that preserve product quality while enhancing energy efficiency.

2 Heat and Mass Transfer in Conveyor Belt Dryers

The drying process in conveyor belt dryers involves complex interactions between heat and mass transfer mechanisms, which govern the moisture removal from wet products. This section explores these mechanisms, highlighting the principles behind heat and mass transfer and their application in different conveyor belt drying systems. The discussion begins with the role of double diffusion. Double diffusion allows mass transfer or moisture release. Initially, moisture diffuses from the product core to the outer layer. The moisture then transfers from the product's surface to the drying agent, which is drier. The heat and mass transfer processes, In Fig. 1, the Fourier law, and Fick's second law of diffusion [7] control heat and mass transfer Eqs. (1) and (2), respectively.

$$q = -k\frac{dT}{dx} \tag{1}$$

$$j = -D\frac{dC}{dx} \tag{2}$$

In normal drying, heat transfer increases the moist/wet product's temperature, enhancing evaporation. Water vapor from the product is transported away by heated air. This continues until the product is dry enough. Product quality degrades as temperature rises. Thus, the best drying procedure should preserve the product's aroma and flavour [6]. Belt drying, suitable for convection or conduction heating, is the most prevalent. Continuous conveyor belt dryers are the most versatile dryers for varied products [6]. Convection heating uses a heat exchanger to heat air or nitrogen, which is then sent to the tunnel or drying chamber where the belt moves the product. This dryer has high throughput and fast drying. Belt motion prevents damp zones and improves product quality [6]. In a conductive refractance window dryer (RWD), shown in Fig. 2, the desired product is made as a thin-film material on a polyethylene conveyor belt. The product is heated by the belt on a circulating hot water bath. After some length, the belt moves on a circulating cooling water bath to cool the product to avoid sticking. This drying method works for heat-sensitive materials but has a specific operational capacity [8]. Tayel et al. [9] reported in their research that the total capacity of RWD was about 0.326 kg/h.

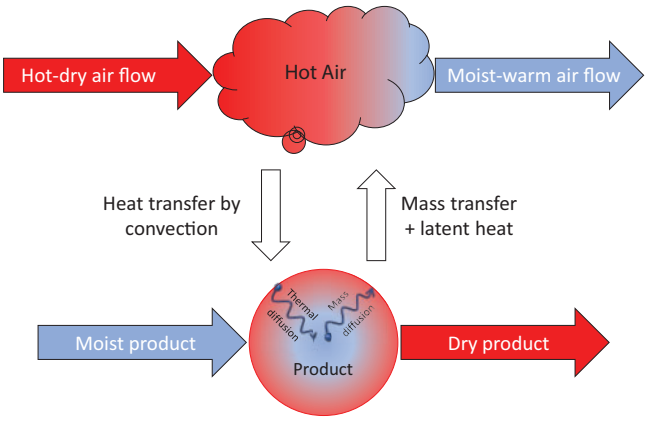

Figure 1: Heat and mass transfer process in convective drying process

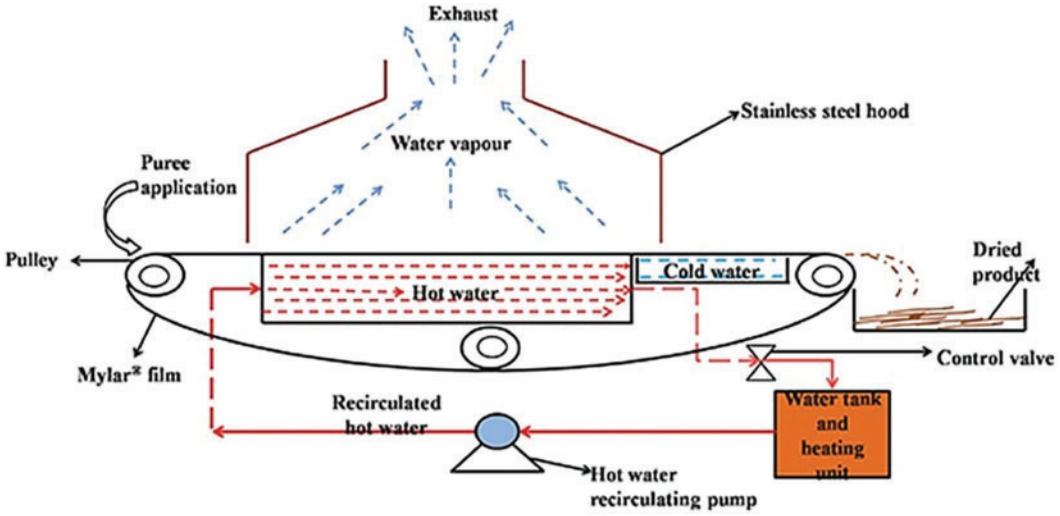

Figure 2: Refractance window dryer [10]

Conveyor belt dryers are integral to many industrial drying processes due to their versatility and efficiency. These dryers consist of a moving belt that transports the product through a drying chamber, where heated air or other drying agents facilitate moisture removal. Conveyor belt dryers, like the one shown in Fig. 3 redesigned to efficiently dry products as they move along a continuous belt through a controlled environment. The image illustrates a typical conveyor belt dryer, featuring a mesh belt, a drying chamber, and temperature controls. Such systems are versatile and widely used for drying various products, especially those requiring uniform drying and consistent quality.

Figure 3: Actual image of conveyor belt dryer [11]

3 Methodology

A comprehensive review of the existing body of literature reveals a consistent stream of research publications focused on developing and improving modelling techniques for conveyor belt dryers. These efforts aim to improve and control the performance of such dryers. Fig. 4 illustrates the number of annual publications on modelling studies generated over the past three decades. The figure is generated by searching for the phrases "Modelling + Conveyor-belt dryer" on various research platforms, including Lens [12], Science Direct [13], and Web of Science [14].

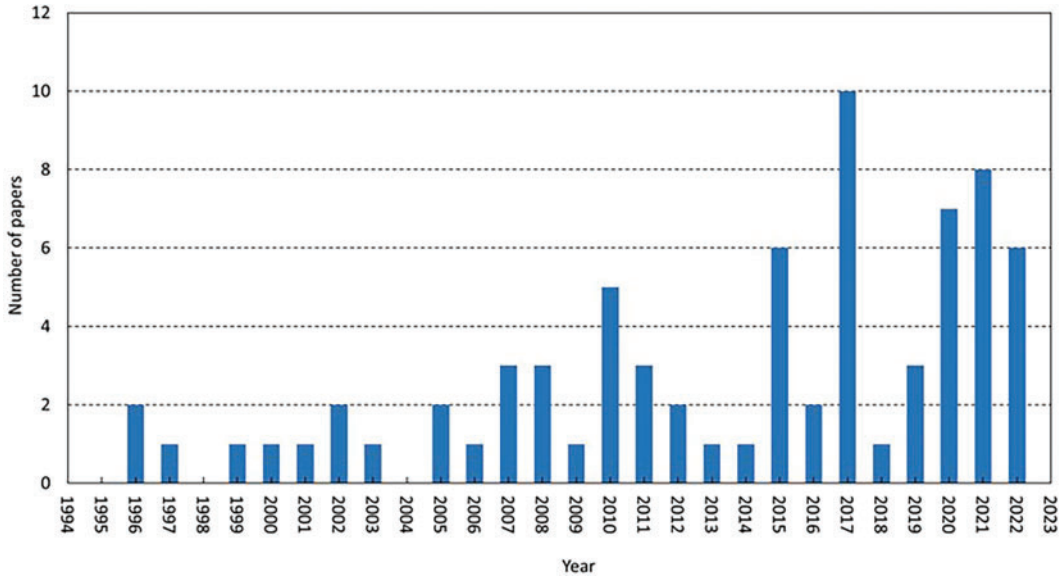

Figure 4: Number of relevant publications each year

These findings demonstrate the extensive number of studies in this field. The total number of publications is then reduced to a set of "relevant articles" through a process of reviewing the titles and the abstracts of the papers in detail. The final set of papers is evaluated through a comprehensive review of each manuscript. The results of the exhaustive examination of relevant scholarly sources

are presented in Table 1. Some of the reviewed papers appeared in more than one search engine, as illustrated in Fig. 5.

Table 1: Results of the comprehensive literature review

	Number of papers	Number of relevant papers	Number of papers within the scope
Lens	1128	204	44
Science direct	1857	63	14
Web of science	119	105	32

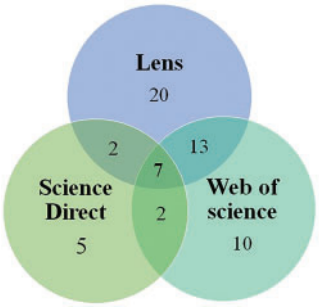

Figure 5: Vin diagram for papers found in the different scientific search engines

An examination of the published research in the field of modelling the drying process in conveyor belt dryers reveals that the predominant methodologies utilized in these studies include theoretical, computational fluid dynamics (CFD), empirical, and performance evaluation of control strategies, as depicted in Fig. 6. The number of publications for each modelling technique is also displayed in Fig. 7. A detailed comparison of the advantages and limitations of each methodology—namely theoretical, CFD, empirical, and control strategies—is presented in Table 2. The methods discussed in this text focus on several aspects of conveyor belt dryer systems, including:

- Design, development, and optimization.
- Performance evaluation using empirical data.
- Control methods.

Both theoretical and CFD modelling are used to design, develop, and optimize the operational parameters. The design of belt dryers and the optimization of the control parameters are topics covered by theoretical modelling methods. Most research on CFD modelling focused on improving the dryer efficiency by homogenizing the airflow distribution. Theoretical modelling and CFD simulations can be either steady or transient. These models can further be categorized as lumped or multidimensional (1-D, 2-D, and 3-D).

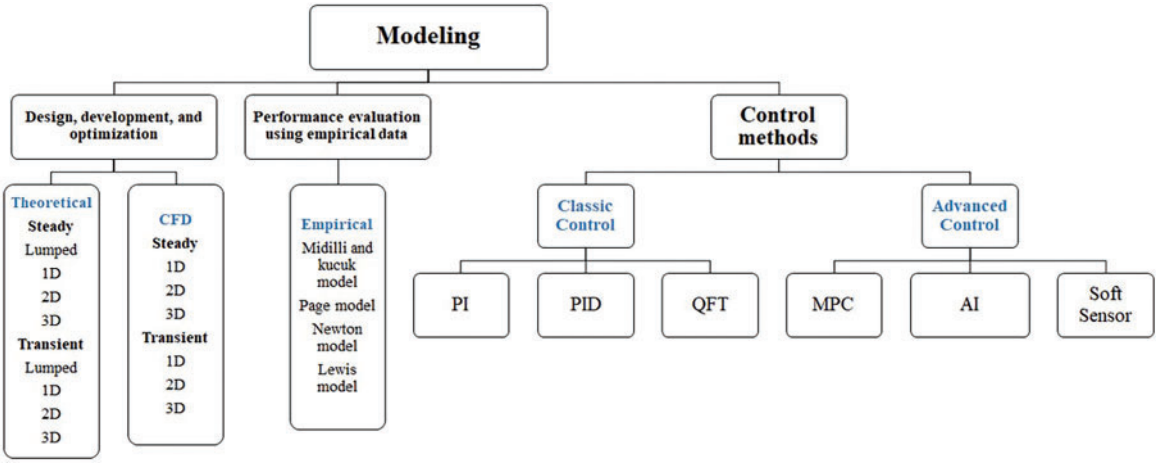

Figure 6: Belt-dryers modelling techniques and the corresponding number of publications for each technique

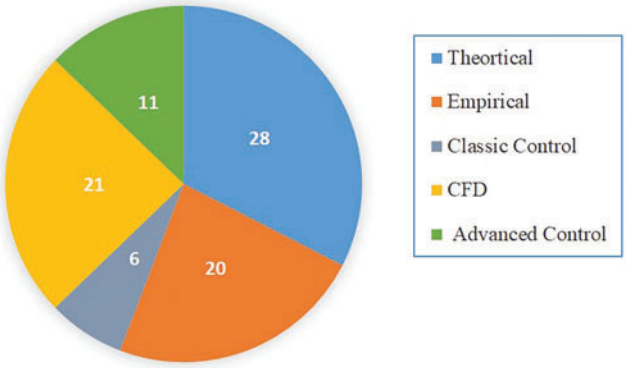

Figure 7: Number of publications of each modelling technique

Table 2: Advantages and limitations of each technique

Technique	Advantages	Limitations	Notes
Theoretical	• Fundamental understanding of physical principles • General solutions and trend prediction • Concise mathematical models	• Simplifying assumptions may not be accurate • Limited scope, may not capture complex phenomena • Requires advanced math skills	• Used to design and optimize belt dryers. • Can be steady-state or transient, lumped or multidimensional (1D, 2D, 3D). • Examples: Modeling heat and mass transfer, predicting drying kinetics.

(Continued)

Table 2 (continued)

Technique	Advantages	Limitations	Notes
CFD	• Simulates complex fluid flow and heat transfer • Detailed insights into flow patterns and temperature • Analyzes a wide range of problems	• Requires powerful computational resources and software • Accuracy depends on models and grid resolution • Time-consuming setup and simulation	• A reliable tool for evaluating belt dryer modeling. • Can be steady-state or transient, 2D or 3D. • Examples: Analyzing airflow distribution, optimizing dryer design.
Empirical	• Provides real-world data • Validates theoretical models and CFD simulations • Identifies trends and relationships	• Limited scope, may not capture all factors • Expensive and time-consuming experiments • Measurement errors and uncertainties	• Used to identify suitable empirical models. • Involves measuring moisture content before and after drying. • Examples: Comparing drying curves to models, using Response Surface Methodology (RSM).
Controllers	• Automates processes, improves efficiency • Maintains system stability and performance • Adapts to changing conditions	• Requires careful design and tuning Susceptible to noise and disturbances • May require significant computational resources	• Used to optimize drying processes and achieve desired outputs. • Can be classical (PI, PID, QFT) or advanced (MPC, AI). • Examples: Controlling moisture content, air temperature, belt speed.

In performance evaluation using empirical data, empirical techniques are utilized to identify the most suitable empirical model, with coefficients, which can accurately represent the performance of the drying process. First, the moisture content of the product is measured pre- and post-drying to compute the overall moisture ratio for the drying process, as described in Eq. (3). Subsequently, several empirical models, such as those based on Midilli et al. [15], Hendreson et al. [16], Newton [17], and Lewis [18], are used to match the overall moisture ratio. Ultimately, the optimal empirical model and its corresponding coefficients are chosen to depict the performance of the drying process accurately. The selection criteria are based on the correlation coefficient (R^2), highest was sought, reduced chi-square (X^2), lowest was preferred, and root mean square error (RMSE). The Response Surface Methodology (RSM) is another empirical technique employed to identify the optimal empirical model. RSM encompasses a range of experimental designs and optimization techniques that aim to elucidate the correlation between a dependent variable and its corresponding independent variables.

$$MR = \frac{X - X_{\mathrm{E}}}{X_i - X_{\mathrm{E}}}, \tag{3}$$

where X is the instant moisture content, X_{E} is the equilibrium moisture content and X_i is the initial moisture content of the product.

Various techniques can be found in the literature that address the control of conveyor belt dryers. Conveyor belt dryers are challenging to regulate because changes in the dryer's intake, such as the inlet solid moisture content, are not immediately apparent at its output. This information delay can considerably affect the performance of the dryer [6]. The controllers used can be classified to

- Classic Control
- Advanced Control

Classical controllers include proportional-integral (PI), proportional-integral-derivative (PID), and quantitative feedback theory (QFT) controllers. QFT is a robust controller technique that can handle plant uncertainty and is developed using robust specifications. Advanced controllers include model predictive controllers (MPC) and artificial intelligence (AI) controllers.

4 Theoretical Modelling Techniques

The review of literature reveals that various researchers have studied drying processes using conveyor belts, fluidized beds, rotary dryers, and belt dryers. Steady lumped models are detailed below in Section 4.1, 1D models are reported in Section 4.2, and a 2-D model is presented in Section 4.3 for belt dryers. Transient modelling of conveyor belts is presented in Section 4.4 for lumped model, in Section 4.5 for 1-D models, and in Section 4.6 for multidimensional models. The results of these studies are summarized in Table 3.

4.1 Steady Lumped Modelling Studies

In 1993, Kiranoudis et al. [19] established a mathematical model for constructing a conveyor belt dryer. The model was used to determine the best flow-sheet structure, building characteristics, and operating conditions with respect to total annual cost. The analysis of the belt structure assumed that the belt dryer was composed of a series of drying chambers and that the drying chamber was an elementary module. The mathematical model was then applied to one elementary module and repeated for the entire dryer. The heat transfer coefficient was assumed to be sufficiently high so that the product and air streams would be in thermal equilibrium at the end of the dryer. The authors used the mass-transfer coefficient reported in Bruin et al. [20]. The proposed methodology implemented to design a drying plant for drying 2400 tons of raw potato per year. To achieve this, the raw material is first cut into 10-mm cubes and then introduced into the processing dryer at a rate of 200 kg of dry solid per hour. The initial moisture content of the raw material is 5 kg of water per kg of dry material (on a dry basis), and the desired moisture content at the dryer's exit is 0.05 kg of water per kg of dry material (also on a dry basis). It is crucial to ensure that the product does not exceed a temperature threshold of 75°C during the drying process to prevent degradation. The maximum available area for constructing the plant's chambers is 5 square meters, and the belt load at the entrance of each drying section is maintained at 50 kg per square meter (on a wet basis).

In 1996, Kiranoudis et al. [21] extended their previous work on conveyor belt dryers to include convective industrial dyers: conveyor belts, fluidized beds, and rotary. Mathematical modelling was used to determine the most effective way to build and run each type of dryer for a given production capacity. The results indicated that the design cost of rotary dryers was higher compared to fluidized

bed dryers. However, in terms of operational efficiency, the situation is reversed due to the superior heat transfer achieved in rotary dryers. On the other hand, conveyor-belt dryers fall somewhere in between, delivering satisfactory results in both design and operation.

4.2 Steady One-Dimensional Modelling Studies

Hosseinizand et al. [22] conducted an economic analysis for a conveyor belt dryer used to of dry microalgae chlorella. Their work focused on the potential for heat regeneration from an adjacent power plant. To identify the crucial design variables, they analytically modelled the belt dryer. An empirical equation for the mass-transfer coefficient was obtained from the experimental data. With the assumption of lumped coordinates for the width and thickness, a 1-D steady-state problem. They used a finite difference approach to solve the system with a convergence criterion of 10^{-5} for the moisture content were at least. Their results indicated that waste heat recovery can be effectively integrated with conveyor belt dryers to reduce the drying costs of Chlorella compared to the other two drying methods.

Sebastian et al. [23] performed a 1-D numerical simulation to analyse a conveyor belt dryer. Their study involved differential relations of the balance equations and transfer functions. Heat and mass transfer networks (HMEN) were developed using the NTU approach, resulting in the formulation of a nonlinear algebraic system of equations. The solution of the nonlinear drying system was obtained by MLTCONV software, employing iterative techniques such as the Newton-Raphson approach. They reported that simulation results using MLTCONV improved computational efficiency compared to traditional methods.

de Souza Barrozo et al. [24] studied the simultaneous heat and mass transfer phenomena in moving bed dryer between air and soybean seeds. A 1-D boundary value problem was developed and solved numerically using a computational algorithm that employed the axial integration differential/algebraic system solver (DASSL) code [25]. Backward differential formula techniques were implemented in the FORTRAN code to solve a broad collection of implicit initial value differential-algebraic equations with a differential index of no more than one. The simulation results were slightly higher when compared to their experimental data, with average variances for air humidity and seed temperature of 3.6% and 2.2%, respectively.

4.3 Steady Two-Dimensional Modelling Study

Holowaty et al. [26] modelled a double pass belt conveyer dryer to dry yerba mate. An experimental setup was constructed to determine the water diffusion coefficient as a function of temperature and moisture content. Then, the analytical equations obtained from the energy and mass balances at each node of the product were reported. Finally, they solved the system of equations using the forward finite difference method. Validation was performed by comparing the experimental results for the same conditions with the mathematical showing RMSE of 0.02, demonstrating that the fit is superior to that of comparable modelling results acquired in the case of a single belt dryer. Simulation results under different drying conditions showed that the dryer's energy efficiency could be improved by recirculating 15% of the exhaust air.

4.4 Transient Lumped Modelling Studies

Vaxelaire et al. [27] developed a numerical model based on experimental laboratory data for drying residual sludge using a belt dryer. They used their experimental data and optimization software to develop a single empirical equation, Eq. (4), which represents the drying kinetics of the sludge. In addition, they used their experimental data to develop an expression for drying potential, Eq. (5), to reduce the set of operating conditions, namely the dry-bulb temperature and relative humidity. The

authors then developed a mathematical model that described the mass and energy balances of the process using the developed empirical equations.

$$Fm_{\mathrm{P}} = \Psi_1 + \left(\frac{\Psi_2}{1+\exp\left(-X/\Psi_4\right)}\right)\left(1-\frac{1}{1+\exp\left(-X/\Psi_3\right)}\right) \tag{4}$$

$$\mathrm{DP} = 1.32\ U_{air}^{0.4}\mathrm{DP}_{th} \tag{5}$$

where Fm_P is the evaporation mass flux density in one pellet, Ψ_i is a set of functions for each sludge, DP is the drying potential, U_{air} is the velocity of air and DP_{th} is the thermodynamic drying potential.

Xue et al. [28] proposed a prediction model to develop the operating parameters of a vacuum belt dryer in which the moisture content of the product during the drying process was predicted using a numerical simulation employing boiling and evaporation models. The numerical simulation was improved by connecting the boiling and evaporation processes with the transient model. Lab-scale and industrial production tests validated the numerical model. The results showed that conveyor belt speed played the most critical role in the vacuum belt dryer process.

Friso [29] proposed mathematical modelling and design guidelines for a conveyor belt dryer. Starting from a simple energy and mass balance on an elementary area of the product, he assumed a temperature distribution inside the dryer and the inlet and exit air temperatures to obtain the heat transfer coefficient. In addition, he assumed that the product temperature was constant during the drying period and was equivalent to the wet-bulb temperature of the incoming air. Moreover, an experimental setup for a pilot-belt dryer was built to validate the proposed mathematical model.

In 2021, Friso [30] optimized his mathematical model in the form of specific two ordinary differential equations (ODEs). The solution of the ODEs performed a relation between the initial and final moisture content and the input and exit air temperatures. Moreover, the experimental model was used to verify the optimized model.

Eng et al. [31] improved the theoretical model developed by Nindo et al. [32] to investigate the temperature gradient of mango puree during the drying process in RWD. For this, a system of partial differential equations with a single product layer and a small-time increment was developed. An experimental model for the RWD was constructed to validate the mathematical model. The model fitted well with the experimental results, showing a p value of less than 0.05, and thus, it can be used to predict the temperatures and heat profiles for the RWD.

Shirinbakhsh et al. [33] designed and simulated a large-scale solar-assisted conveyer-belt dryer for biomass drying using a numerical model implemented in MATLAB [34]. The design parameters from their numerical model were used to perform economic optimization. Their model was verified by comparing the drying time obtained to that of drying gelatine and carrot in the conveyor belt dryer obtained using correlations from [35] and [36]. In their numerical model, the authors used empirical equations for the equilibrium moisture content, the drying time constant, and the drying time, as shown in Eqs. (6)–(8), respectively.

$$X_e = b_1 \exp\left[\frac{b_2}{273+\mathrm{T}}\right]\left[\frac{\mathrm{a_w}}{1-\mathrm{a_w}}\right]^{\mathrm{b_3}} \tag{6}$$

$$\mathrm{t_c} = \mathrm{c_0\ d^{c_1} V^{c_2} T^{c_3} Y^{c_4}} \tag{7}$$

$$\mathrm{t} = -\mathrm{t_c \ln}\left[\frac{\mathrm{X}-\mathrm{X_e}}{\mathrm{X}_i-\mathrm{X_e}}\right] \tag{8}$$

where X_e is the equilibrium moisture content of the product, b_1, b_2, b_3 are feed properties, T is temperature of feed, a_w is water activity. t_c is the drying time constant. d is the material diameter. V, T and Y are drying air velocity, temperature, and absolute humidity, respectively. c_0, c_1, c_2, c_3 and c_4 are the constant factors of the equation and X_i is the initial moisture content.

A genetic algorithm was used to carry out the economic optimization, under different economic scenarios to minimize the total annual cost (TAC) for the solar-assisted conveyer-belt dryer. The significant variables that affect the economic analysis were identified using the degrees-of-freedom analysis. Based on which, the system's capital and operating costs were calculated. It was shown that low solar fraction scenarios resulted in an infeasible alternative compared with the fossil fuel dryers.

4.5 Transient One-Dimensional Modelling Studies

Canabarro et al. [37] studied the effects of drying conditions on the olive leaf supercritical extracts' composition. They developed a mathematical model, based on energy and mass balances, to predict both temperature and moisture content of the leaf. The mass transfer coefficient and the convection heat transfer coefficient were estimated by fitting the experimental data with a mathematical model using the least squared method. The results suggested that drying on a conveyor belt dryer is an appealing alternative to dry leaves aimed at supercritical extraction.

Mirzahoseinkashani et al. [38] proposed a mathematical model to study the crossflow conveyor belt dryer. The developed model was a function in moisture content, as presented in Eqs. (9) to (11), The model was based on the finite-volume method. Finally, they used MATLAB, version 7 [34] to implement a computational code and obtained numerical results. The results of the moisture content were compared to experimental data of the fixed bed to validate the methodology. Consideration of the porosity variation by the grain moisture content resulted in more accurate results from the mathematical modelling proposed.

$$\rho_{\text{product}} = 1353 - 179.4\text{X} + 78.4\text{X}^2 \tag{9}$$

$$\beta = 0.513 - 0.11\text{X} + 0.48\text{X}^2 - 0.56\text{X}^3 \tag{10}$$

$$A^* = 729\text{X}^2/\text{X}^3 \tag{11}$$

where $\rho_{product}$ is the density of the product, β is the material porosity and A^* is the specific surface area.

De Holanda et al. [39] performed a mathematical model that describes the drying process of the silkworm cocoon in a conveyor belt dryer. The authors used the changing parameters, as specific heat, density, and relative humidity, developed by Jumah et al. [40], and Rossi [39]. The heat transfer coefficient was obtained from Incropera 2002 [41]. They used the finite-volume method to discretize the equation system by integrating them over the control volume and time. The system was solved by generating a computational code using Mathematica [42]. The validation was done by comparing the numerical results of moisture content with the experimental results of fixed bed reports which obtained no errors.

Salemović et al. [43] posed a mathematical model for drying of thin layer of potatoes in a conveyor belt dryer. They studied the process with the assumption that the layers of the moist potatoes were separated into segments. Each segment had its own drying agent, heater, fan, and belt velocity. The model was made in the form of four non-linear partial differential equations. The equations were transferred to two ODEs with constant coefficients, Eqs. (12) and (13). This is in addition to an extra equation of a transcendent character, Eq. (14). These equations were solved numerically by the Euler method of simple finite differences. The obtained results using the developed mathematical model

provided a clear image for the variation of moisture and temperature in the thin layer of the material.

$$\frac{\mathrm{d}X_{\mathrm{product}}}{\mathrm{d}\eta} = -\frac{\mathrm{k_m}S_{\mathrm{m}}}{U_{\mathrm{product}}\rho_{\mathrm{dp}}}\left[p_{\mathrm{wvs}} - R_{\mathrm{wv}}\rho_{\mathrm{Dair}}\mathrm{X}_{\mathrm{air}}\left(T_{\mathrm{air}} + T_0\right)\right] \tag{12}$$

$$\frac{\mathrm{d}T_{\mathrm{product}}}{\mathrm{d}\eta} = \frac{\mathrm{h_m}S_{\mathrm{m}}}{U_{\mathrm{product}}\rho_{\mathrm{dp}}\left(c_{\mathrm{dp}} + X_{\mathrm{product}}c_{\mathrm{product}}\right)}\left(T_{\mathrm{air}} - T_{\mathrm{product}}\right) - \frac{\mathrm{k_m}S_{\mathrm{m}}}{w_{\mathrm{m}}\rho_{\mathrm{dp}}\left(c_{\mathrm{dp}} + X_{\mathrm{product}}c_{\mathrm{water}}\right)}\left[p_{\mathrm{wvs}} - R_{\mathrm{wv}}\rho_{\mathrm{da}}\mathrm{X}_{\mathrm{air}}\left(T_{\mathrm{air}} - T_0\right)\right]\left(r_0 - K_{\mathrm{r}}T_{\mathrm{product}}\right) \tag{13}$$

$$A\left(\frac{X_{\mathrm{product}}}{X_{\mathrm{product}}I}\right)^{a_1}\left(\frac{T_{\mathrm{product}}}{T_{\mathrm{product}}I}\right)^{a_2}\left\{X_{\mathrm{product}} - \left[\frac{-\ln\left(1 - \frac{p_{wvs}}{p_1 10^{\frac{p_2 T_{\mathrm{product}}}{p_3 + T_{\mathrm{product}}}}}\right)}{k_1\left(T_{\mathrm{product}} + T_0\right)^{k_2}}\right]\right\}^{\frac{1}{k_3\left(T_{\mathrm{product}} + T_0\right) + k_4}} = \frac{k_{\mathrm{m}}S_{\mathrm{m}}}{\rho_{\mathrm{dp}}}\left[p_{\mathrm{wvs}} - R_{\mathrm{wv}}\rho_{\mathrm{Dair}}X_{\mathrm{air}}\left(T_{\mathrm{air}} + T_0\right)\right] \tag{14}$$

where $X_{product}$ is the moisture content of the product, k_m is the mass transfer coefficient, η is a space co-ordinate, X_{air} is the absolute humidity of air stream, S_m is the specific surface area of evaporation (surface/volume) (m^2/m^3), K_r is a constant, r_0 is the latent heat of evaporation of water at 0 (°C) and k_{1-4}, a_{1-2}, A are constants.

Faggion et al. [44] investigated mechanisms for heat and mass transfer coefficients of ilex paraguariensis during drying in cross flow conveyor dryer. The value of biot (Bi) numbers and the corresponding rates of heat and mass transfer impacted the entire analysis. The mechanism was obtained analytically by solving Fick's second law as well as heat transfer from the chart of Heisler or in a long cylinder with finite surface resistances. Experimental setup was used to validate the model. Their modelling results were able to agree well with the experimental data.

Schmalko et al. [45] proposed a mathematical model to evaluate the temperature and moisture content of yerba mate leaves and twigs during the drying process. The model was solved using the finite difference method. The model was validated using experimental data obtained at the factory. The predicted values of moisture and chlorophyll content were in good agreement with the experimental data with RMSE value equals to 0.0033.

Burmester et al. [46] focused on heat and mass transfer of coffee during drying in a vacuum belt dryer. They built an experimental model to investigate the thermal conductivity and influence of the porosity of coffee. Based on these experimental results a numerical model was developed to clarify the coupled heat and mass transfer.

Pang et al. [47] developed a mathematical model to simulate the drying process of wood chips in a moving bed dryer. A system of equations was solved numerically to calculate the changes in moisture and temperature with respect to the location along the dryer length and through the bed thickness. Moreover, it was validated by the experimental data they obtained from their experimental model.

Neto [48] developed a detailed continuous, conveyor belt dryer simulator. Then to reduce the production cost and meet production specifications, they optimized the operating parameters, including drying air velocity and drying air temperature. The system of equations is composed of

two parts, the equations describing the distributed mass and energy balance around the food particle and the mass and energy balance describing the drying air. The first subsystem was solved using the Method of Lines (MOL). The MOL modifies an Initial Value Partial Differential Equation (IV-PDE) into a system of coupled First-Order ODE. The second one was solved by the Fourth Order Runge-Kutta method, since this is a set of non-stiff Ordinary Differential Equations.

4.6 Transient Multi-Dimensional

Ostrikov et al. [49], used a hybrid approach for modelling the drying process of tube-shaped pasta. They started with an empirical equation for the drying time and mass transfer by Dzhamasheva [49]. The authors then simplified the detailed energy and mass transfer equations which resulted in a set of ODEs, as shown in Eqs. (15)–(19). Then they were solved numerically by the fourth order Runge-Kutta method.

$$(\Delta X)_n = \frac{1}{h}\left(\frac{\partial X_n}{\partial Z} - \frac{X_n - X_{n-1}}{h}\right) + \frac{1}{Z_n}\cdot\frac{\partial X_n}{\partial Z} \tag{15}$$

$$\frac{dX_1}{dx} = \mathrm{Lu}\left(\frac{3n^2}{2R^2}X_{k+1} - \frac{3n^2}{2R^2}X_k\right) \tag{16}$$

$$\frac{dX_k}{dx} = \mathrm{Lu}\left(\frac{n^2\,(2k+1)}{2R^2k}X_{k+1} - \frac{2n^2}{R^2}X_k + \frac{n^2\,(2k-1)}{2R^2k}X_{k-1}\right)$$

$$k = 2, \ldots, n-1 \tag{17}$$

$$\frac{dX_n}{dx} = \mathrm{Lu}\left(2n^2\,(X_{n-1} - X_n) - (2n-1)\mathrm{Bi}_m^{'}X_n\right) \tag{18}$$

$$\frac{\partial T}{\partial x} = -\mathrm{Nu}^{'}T + \mathrm{KoBi}_m^{'}X_n \tag{19}$$

While ΔX represents the loss of evaporated moisture and X_n represents the moisture content in the nth particle.

Koop et al. [50] presented a transient two-dimensional model used to investigate the drying of mate leaves in a deep bed dryer. They modified their earlier transient model [51] that focused on thin layer drying in the conveyor belt. The mathematical modelling combined the dependable thin-layer continuous differential equation subsystem with a partial subset of partial differential equations (PDEs). Moreover, empirical equations of the heat and mass transfer coefficient for different products were developed, in terms of bed porosity, density of the product, moisture content of the product, and air properties (density and humidity). The two-dimensional model was modelled as a set of ODEs solved numerically using the Euler method using MATLAB version 6.1 [34]. Their model was verified experimentally. Sorokovaya et al. [52] proposed a mathematical model and optimization for the drying of thermolabile materials. The model investigated phase changes in colloidal capillary-porous materials as well as heat and mass transfer. The system of differential equations was solved numerically using an explicit three-layer difference mesh of Nikitenko [53]. To assess the accuracy and effectiveness of the mathematical model and numerical method that were developed, they conducted a comparison between the results obtained from a numerical simulation using these tools and the results obtained from a physical experiment. The calculated results closely align with the corresponding experimental data, with a maximum error of only 2.2%.

Table 3: Modelling results of theoretical papers

Author	Dried product	Objectives	Results	Validation method or verification approach
Kiranoudis et al. 1994 [19]	Potato	Developing a mathematical model for design optimization of conveyor belt dryers based on flow-sheet structure, construction characteristics, and operational conditions.	Lowest total annual cost which was 122,000 US dollars, split between capital costs (42%) and operational requirements (58%).	The document lacks a comprehensive validation process, which would involve comparing model predictions to experimental data and performing sensitivity analyses. It partially addresses validation by applying the model to a specific case study.
Kiranoudis et al. 1996 [21]	Potato	Design and compare the performance of three industrial dryers in terms of total annual cost for a given production capacity. Conveyor-Belt Dryer: this was based on a two-section dryer with conveyor belt area from 17 to 34 m^2 and air flow rate from 25,000 to 144,000 m^3/h. Fluidized-Bed Dryer: 2.2 m diameter structure with air flow rate of 55,700 m^3/h. Rotary Dryer: 13.7 m long with air flow rate of 40,000 m^3/h.	A study showed that the rotary dryer, despite being more expensive to design initially, offers operational advantages in terms of favoured heat transfer. The rotary dryer has the lowest fuel consumption among the three types of dryers discussed, resulting in a lower total annual cost compared to the fluidized-bed dryer. However, it is important to note that the conveyor-belt dryer lies between the rotary dryer and the fluidized-bed dryer in terms of both design and operation, providing satisfactory results. Conveyor-Belt Dryer Fuel Consumption: 62.2 and 10.8 kg/h. Total Annual Cost: $38,400/yr Fluidized-Bed Dryer: Fuel Consumption: 179.7 kg/h. Total Annual Cost: $44,200/yr Rotary Dryer: Fuel Consumption: 61.5 kg/h. Total Annual Cost: $57,200/yr.	The paper presents two case studies where the models are applied to specific scenarios. While not a rigorous validation, these case studies demonstrate the models' ability to generate realistic results and provide insights into dryer design and operation. The authors perform sensitivity analyses to assess the impact of parameter variations on the predicted optimal cost. This helps to understand the model's behavior and identify critical parameters.
Hosseinizand et al. 2017 [22]	Microalgae	Estimate the cost of drying microalgae using waste heat from an industrial source and analyse the economics of drying microalgae in a conveyor belt dryer compared to other drying methods including an assessment of the impact of integrating waste heat recovery on drying costs.	The cost of drying microalgae from 55% to 10% moisture content ranges from $46.13 to $109.64 per ton of dried product, influenced by the Hand factor (ratio of installed cost to purchased cost). Natural gas at $6.27/GJ increases the drying cost to $83.47 per ton (with a Hand factor of 1). Commercial spray drying of microalgae costs $109.05 per ton of dried product (with a Hand factor of 1).	The paper lacks a dedicated section on model validation and verification, the authors employ a combination of approaches to ensure their model is reliable and accurate. These approaches include grounding the model in established theory, using experimental data to derive key parameters, comparing predictions with industrial data, and performing sensitivity analyses.
Sebastian et al. 1996 [23]		Presenting a new approach to designing conveyor belt dryers using heat and mass exchange networks by applying the Number of Transfer Units (NTU) method and network theory in the design and analysis of multiple-conveyor dryers.	The proposed NTU method combined with network theory accurately represents drying processes. They successfully simulated multiple conveyor dryers in steady-state conditions and static dryers in non-steady-state conditions.	The paper doesn't explicitly outline a separate validation and verification process, it provides evidence that the models were developed based on existing knowledge and evaluated through optimization studies, and some functions from experimental data as drying rate and mass transfer coefficient.

(Continued)

Table 3 (continued)

Author	Dried product	Objectives	Results	Validation method or verification approach
Barrozo et al. 2006 [24]	Soybean seeds	Studying the simultaneous heat and mass transfer between air and soybean seeds in moving bed dryers with parallel flow (concurrent and counter current) to verify the validity of classical assumptions and investigate the influence of non-flat fluid velocity profiles.	The average deviations for air humidity and seed temperature between the simulated results and experimental data are 3.6% and 2.2%, respectively.	As discussed in the results section, the researchers validated their theoretical model by building experimental dryers and comparing simulated results to experimental data, finding average deviations of 2.2% for seed temperature, 3.6% for air humidity, and 2.0% for seed moisture content, generally within the range of experimental uncertainties. They also considered wall effects and used established correlations to enhance the model's rigor and avoid overfitting.
Holowaty et al. 2020 [26]	Yerba mate	Developing a numerical model of a double deck dryer used for drying yerba mate to improve the energy efficiency of the drying process.	The energy efficiency of a conveyor belt dryer operating with hot air at 100°C and a solids mass flow rate of 4000 kg/h can be improved from 40% to 63.70% by recirculating 15% of exhaust air. Increasing the solids mass flow rate to 6200 and hot air temperature to 120°C results in 46.21% drying efficiency.	The researchers validated their model by comparing simulated results to experimental data collected from two small-scale industrial dryers. They measured gas temperature at the inlet, between the two belts, and at the outlet using PT100 thermocouples. The comparison between model predictions and experimental data showed a good fit, with RMSE values of 0.020 for moisture content, 0.004 for air humidity, and 9.5 for air temperature.
Vaxelaire et al. 2002 [27]	Residual sludge	Studying and analysing the drying kinetics of residual sludge, with a focus on designing and simulating a belt dryer to improve the understanding of the drying process and provide insights into the relevant parameters and phenomena involved.	The results indicated that a conveyor belt dryer is not well suited for drying activated sludge due to the formation of a crust. The belt dryer is more efficient for drying PVC sludge due to its ability to dry with reasonable residence times.	The researchers conducted extensive experiments to characterize the drying kinetics, crust formation, shrinkage, particle size, specific heat capacity, and sorption isotherms of two types of sludge: activated sludge and PVC sludge. This experimental data served as the foundation for developing the core of their drying model. However, the paper primarily focuses on the model's qualitative validation, comparing simulated trends to experimental observations rather than providing specific quantitative measures of model fit.

(Continued)

Table 3 (continued)

Author	Dried product	Objectives	Results	Validation method or verification approach
Xue et al. 2022 [28]	Licorice	Developing a novel method for optimizing the vacuum belt drying process of licorice extract using numerical simulation and determining the optimal operating conditions for drying licorice extract with the desired final moisture content.	Developed and validated numerical simulation model for the vacuum belt drying process of licorice extract with MSE ranging from 2.176×10^{-5} to 6.58×10^{-3} for lab-scale and industrial production experiments, respectively.	The theoretical model was validated using two sets of experiments: • **Lab-scale experiments:** These were performed in a vacuum drying oven to simulate the VBD process under controlled conditions. The licorice extract was heated at different temperatures and for different durations, and the final moisture content was measured. • **Industrial production experiments:** The model was also tested in a real-world industrial VBD setting. The moisture content of the licorice extract was measured at the end of the drying process and compared to the model's predictions. The results from both the lab-scale and industrial production experiments showed good agreement with the predictions of the theoretical model.
Friso 2020 [29]	Alfalfa	Developing correlations between several parameters, including air and product flow rates, enthalpies, temperatures, and belt diameters to optimize dryer design.	The mathematical model provides guidelines for designing conveyor-belt dryer with tangential flow using developed relationships between intensive quantities (temperatures, humidity, and enthalpies), extensive quantities (air and product flow rates), and dimensions (length and width of the belt).	The theoretical model was validated using experimental data collected from a pilot dryer. The pilot dryer was set up to simulate the conditions of a conveyor-belt dryer with tangential flow, and alfalfa was used as the test product. The experimental results also confirmed the validity of the mathematical model and the design guidelines, with an error of 2.6%. This indicates that the model can accurately predict the final moisture content of the product and can be used to optimize the dryer design and operating parameters for improved efficiency and product quality.

(Continued)

Table 3 (continued)

Author	Dried product	Objectives	Results	Validation method or verification approach
Friso 2021 [30]	Alfalfa	Developing mathematical models and guidelines for the design and process adjustment of a conveyor-belt dryer with tangential flow to optimize the design of the dryer to better preserve the organoleptic (sensory) and nutritional qualities of the dried food product. The models were established based on ordinary differential equations (ODEs) that relate the final moisture content of the product, the outlet air temperature, and other quantities.	Established an enhanced control system based on ODEs that uses measured exit temperatures to establish moisture content.	The theoretical model was experimentally verified using a pilot drying plant. The plant was used to dry alfalfa stems (with leaves) that were cut into 5 cm long pieces. The experiment involved setting two different conveyor-belt speeds and two different air temperatures at the inlet. The researchers measured the mean values of the air temperature at the input (TAI) and the exit (TAE) of the dryer, as well as the alfalfa final moisture content at the exit of the dryer (XF). The experimental results were compared to the values calculated from theoretical data. The comparison showed some discrepancies, especially for the low values of the moisture content. These errors were attributed to the simplifying assumptions made during the mathematical development, such as the dryer being adiabatic and the thermal energy necessary to heat the dry mass of the product from TPI to TWB being negligible. To account for these factors, a corrective coefficient was introduced.
Eng et al. 2011 [31]	Mango purees	Investigating the product temperature and heat transfer in electrically heated Refractance Window (RW) dryers, to better predict the temperature of puree during RW drying.	Experimental and simulated results demonstrated a strong correlation ($p < 0.05$) between plastic sheet and product temperatures. While a slight discrepancy was observed between the predicted (93.9°C) and measured (94°C) temperatures of the plastic conveyor base immersed in water, both values fell within the range of 91°C to 93°C. The disparity between the water temperature (96°C) and the mean surface temperature of the plastic conveyor (92°C) was likely due to heat losses through the stainless-steel base. During the brief drying process in the RW pilot dryer, the temperature of the mango puree on the plastic conveyor varied from 72°C to 86°C at a speed of 0.0065 m/s and from 64°C to 84°C at a speed of 0.0078 m/s.	The theoretical model was validated using experimental data obtained at MCD Technologies, Inc. in Tacoma, WA, USA. The experiments involved drying mango puree using a pilot-scale RW dryer and measuring various parameters like temperatures of water, air, plastic conveyor, and product. The model's predictions for the temperatures of the Mylar plastic sheet and the mango puree during the drying process were compared with the experimental measurements.

(Continued)

Table 3 (continued)

Author	Dried product	Objectives	Results	Validation method or verification approach
Shirinbakhsh et al. 2017 [33]	Biomass	Designing a solar-assisted conveyer-belt dryer for biomass and optimize its performance.	The drying air's temperature and velocity have the greatest impact on TAC (Total Annual Cost). A 10% drop in drying air temperature leads to only 238$ (0.8%) increase in TAC. TAC is particularly sensitive to temperature and moisture levels in dry air. For every 10% change in the drying air moisture leads to less than 350$ (0.6%) in the TAC.	The theoretical model was validated using data from previously published studies on conveyor-belt dryers. The drying time for gelatin and carrot, as reported in these studies, was compared to the values predicted by the implemented code. The results showed less than 9% error, indicating that the model can accurately predict the drying time for different materials.
Canabarro et al. 2019 [37]	Olive leaves	Investigating the impact of operating parameters on the composition of supercritical extracts obtained from olive leaves using a conveyor belt. Developing and validating a model based on mass and energy balances to describe the drying process.	The extraction kinetics of the bioactive compounds from the olive leaves were not substantially affected by the operating parameters, including air temperature and residence time. The extraction yield of the bioactive compounds was improved for samples dried at 50°C for 180 min.	The model's was validated against measured values based on residence times in the dryer ranging from 60 min (one conveyor pass in the dryer) to 180 min (three conveyor passes). The results showed that the model was able to predict the measurement well, with an $R^2 > 0.93$ between for all drying conditions for the output moisture. This indicates that this simplified approach offers good predictions.
Mirzahosein kashani et al. 2008 [38]	Grains	Developing a mathematical model that correlates bed porosity and transient terms in the drying process of a crossflow conveyor belt dryer to predict the humidity ratio, air temperature, moisture content, and material temperature throughout the drying process.	The developed model can predict humidity ratio, air temperature, moisture content, and material temperature throughout the drying process. The residence time of the primary model equals to 4357 s while the modified model equals to 4674 s.	The model was validated by comparing the numerical results of the average moisture content of the grain with experimental data for fixed bed drying. This comparison was considered valid because the velocity of the conveyor belt is much smaller than the air velocity.
Holanda et al. 2005 [39]	Silkworm cocoon	Studying the drying conditions of silkworm cocoons to optimize the process and improve energy efficiency using a mathematical model considering thermo-physical properties, porosity of the bed, and transient terms in the drying and heating kinetics.	The average moisture content obtained from the numerical results is compared with experimental data, showing good agreement.	The model was validated by comparing the numerical results of the average moisture content of the cocoons with experimental data for both fixed bed drying and continuous drying. The experimental setup wasn't explicitly described in the document, but it mentions using data from Lima [53] for validation. The comparison with fixed bed drying data was considered valid because the velocity of the conveyor belt is much smaller than the air velocity. In both setups, measurements of the moisture content of the cocoons were taken at different time intervals during the drying process. These experimental data points were then compared with the predictions of the numerical model.

(Continued)

Table 3 (continued)

Author	Dried product	Objectives	Results	Validation method or verification approach
Salemović et al. 2015 [43]	Potatoes	Analysing the drying kinetics of potatoes and similar natural products and provide insights that can be useful for predicting and controlling the drying process using a mathematical model.	The presented mathematical model is considered suitable for automated control systems. It implies that the model can be employed to develop control strategies for regulating and optimizing the drying process in a conveyor-belt dryer.	The paper did not explicitly detail the validation methods used for the theoretical model.
Faggion et al. 2016 [44]	*Ilex paraguariensis*	Investigating the mechanisms of heat and mass transport during the drying of mate twigs in a crossflow thin-layer conveyor dryer by relating the resistance of mass and heat transfer to the Biot numbers during the drying process.	The results indicated that convection played a more significant role than conduction in heat transfer, as evidenced by low estimated Biot numbers (<0.55). Analysis involving a convective mass transfer coefficient revealed high mass-transfer Biot numbers ($\approx 5.37 \times 10^3$ to 3.65×10^5), indicating that diffusion governed the drying of twigs.	The researchers validated their theoretical model by comparing its predictions with experimental data, performing sensitivity analysis (Biot numbers), and tuning model parameters. The experimental setup involved a conveyor-belt dryer with controlled temperature and airflow, and measurements of both twig surface temperature and moisture content over time.
Schmalko et al. 2007 [45]	Yerba mate (*Ilex paraguariensi*)	Evaluating temperature and moisture content in leaves and twigs of yerba mate in an industrial flow-through dryer by modelling heat and mass transfer to estimate chlorophyll losses and validate the model against experimental data.	The experimental measurements and predicted values of moisture and chlorophyll content agreed well (RSME for moisture content were lower than 0.1178 for twigs and 0.0033 for leaves).	The primary method for validating the model was by comparing its predictions of temperature and moisture content with experimental measurements taken at the factory. This involved measuring the temperature and moisture content of leaves and twigs at different levels within the dryer bed and comparing these values to those predicted by the model. The authors further validated the model by using the predicted temperature and moisture profiles to estimate chlorophyll losses in the leaves. Chlorophyll degradation is sensitive to temperature and moisture content, so accurate prediction of these variables would lead to accurate chlorophyll loss estimations. The estimated chlorophyll losses were then compared with experimental measurements of chlorophyll content at the dryer outlet. To quantify the agreement between the predicted and experimental values, the authors calculated the RMSE for both moisture content and chlorophyll retention. This statistical measure helped assess the overall accuracy of the model.

(Continued)

Table 3 (continued)

Author	Dried product	Objectives	Results	Validation method or verification approach
Burmester et al. 2012 [46]	Coffee	Investigating heat and mass transfer during the drying of liquid pasty plant extract using vacuum belt drying to optimize the drying process.	Drying at low pressure (1–15) mbar leads to series of drawbacks, the volume of the coffee extract increases and so the thermal conductivity decreases leading to slower drying process, higher pressure will make the product more desirable.	The authors validated their numerical model by comparing the predicted temperature and dry matter content evolution with the experimental data obtained from the lab-scale vacuum belt dryer. While the general trends were in good agreement, some deviations were observed, particularly at the dryer inlet and in the regions between the heat exchangers. These discrepancies were attributed to limitations in the measurement method and assumptions made in the model, such as adiabatic boundary conditions between heat exchangers.
Pang et al. 2010 [47]	Woody biomass	Developing a mathematical model for the packed moving bed drying process of woody biomass to optimize the drying operation.	Overall drying time of the woody chips took 35 min: starting with 8 min of temperature increase followed by fast drying. The results indicate that optimized drying can be achieved by using a counter current reversed flow configuration, allowing for the use of lower air flow rates to achieve the desired drying.	
Neto 1997 [48]	Potato	Developing mathematical models and simulation techniques to describe the drying process in a dryer to optimize drying performance.	The results reveal a significant discrepancy between current and optimal operating conditions for drying. Optimal air velocity drops from 1.27 to 0.822 m/s, while temperature remains near optimal at 354.7 K compared to the current 355.6 K. Notably, implementing these adjustments drops drying cost from $0.1453/s to a mere $0.0936/s, representing a substantial 35% reduction in operational expenditure.	The researchers used experimental data to validate their theoretical model. They used a tunnel dryer to conduct their experiments. The tunnel dryer was used to dry both fresh, wet chips and water-soaked chips. They compared the predicted moisture content and temperature profiles to the experimental data. The results showed that the model was able to accurately predict the drying behavior of the wood chips.
Ostrikov et al. 2021 [49]	Pasta	Creating a model that accurately describes the drying process to optimize the drying process by minimizing heating costs while maintaining the quality of the dried product.	The mathematical model accurately predicted drying behaviour with an absolute deviation below 12.5%. This model guided the design of a unique conveyor dryer with stepwise heat supply. The optimal air velocity for minimum cost was found to be 0.822 m/s, significantly lower than the tested range.	The researchers used experimental data to validate their model. They compared the predicted moisture content and temperature profiles to the experimental data. The results showed that the model was able to accurately predict the drying behavior of the pasta, with an absolute deviation below 12.5% as mentioned in results.

(Continued)

Table 3 (continued)

Author	Dried product	Objectives	Results	Validation method or verification approach
Koop et al. 2015 [50]	Mate leaves	Proposing a transient two-dimensional model for deep-bed drying of Mate leaves in a single-pass, single-zone conveyor-belt dryer.	The results of the study indicate that the proposed drying model successfully predicted the experimental data for both corn and rough rice drying in batch dryers. The model accurately described the behaviour of air temperature, moisture content, and absolute humidity at various positions within the dryers.	The validation of the proposed model relies on a comparison between its predictions and experimental data under steady-state and transient conditions. For steady-state validation, drying experiments were conducted using different bed depths of mate leaves (0.05, 0.10, and 0.15 m) in a conveyor-belt dryer, with inlet drying temperatures set to approximately 39°C, 47°C, and 53°C. The model's ability to capture air and solid temperatures at the top of the beds, as well as the average moisture content, demonstrates its reliability under stable operating conditions, as there was good agreement between experimental observations and model predictions.
Sorokovaya et al. 2019 [52]		Developing a mathematical model and numerical method for simulating the heat and mass transfer, as well as phase transformations, in colloidal capillary-porous materials during continuous drying in a belt dryer to optimize the drying process of thermolabile materials.	The convective-condensation method was proposed as an efficient approach to decrease drying time and energy consumption while maintaining product quality. The results of the numerical simulation were compared with experimental data, showing good agreement with a maximum error of 2.2%.	The theoretical model was validated and verified through comparison with experimental data. The authors conducted experiments using a laboratory-scale conveyor belt dryer to collect data on the drying kinetics of a table beet under controlled conditions. The experimental setup involved a thin layer of table beet placed on the conveyor belt, subjected to a hot air stream with controlled temperature and humidity. The moisture content and temperature of the table beet were measured at different time intervals. The experimental data were then compared with the predictions of the theoretical model. The authors reported good agreement between the experimental and predicted values, indicating the validity of the model in capturing the essential features of the drying process.

5 Computational Fluid Dynamics

CFD is considered as a reliable tool for evaluating the modelling of belt dryer in food applications. Steady 2-D CFD models are reported in Section 5.1 and 3-D CFD models are presented in Section 5.2. Transient 1-D CFD model is presented in Section 5.3, while 2-D CFD models are reported in Section 5.4, and 3-D CFD modelling technique was reported in Section 5.5. A summary of these

studies is presented hereinafter and a summary of the findings from these studies can be found in Table 4.

5.1 Steady Two-Dimensional

Khankari et al. [54] used the finite-volume method to develop steady 2-D numerical CFD model for a double-deck conveyor dryer. They used their model to evaluate the performance of a moving bed dryer. The governing equations illustrate the conservation of momentum, heat, and moisture in the computational domain. The momentum source term represented the air side pressure drop, while that in the energy equation for air side represented the thermal energy exchange with the product. The source term in the air moisture equation represented the moisture exchange with the product. Their numerical model was solved using the finite volume method which was implemented through the adaptation routine of a general-purpose CFD code designed by Innovative Research Inc, Plymouth, MN.

Böhner et al. [55] used FLUENT [56] using the (k-ε) standard turbulence model, to study the addition of guide vanes, with different flap angle as an improvement to the distribution of the air flow inside a belt dryer. An experimental model was also built to support the CFD model by measurements. By adjusting the flap setting to 45°, the moisture content became more similar on both sides at different belts. Furthermore, after installing inclined roof-style air guiding plates below the first belt, the hot air from the sides reached the middle of the belt, leading to improved and more uniform drying across the belt. With the air guiding plates, the moisture content ranged from 65.4% to 74.1% wet basis (w.b.) at the end of the first belt and between 3.7% and 4.2% w.b. at the end of the fifth belt.

5.2 Steady Three-Dimensional

Zhang et al. [57] used ANSYS Fluent [56], version 16.0, using the (k-ε) standard turbulence model, to study the air distribution in a belt dryer. The CFD model evaluated five different product thicknesses. A finite volume method with porous media formulation was used in the simulation. Their numerical model was validated experimentally using extruded fresh catfish feed. There was negligible difference observed between the simulated values and the experimental values.

Mondal et al. [58] used ANSYS Fluent [56], version 16.0. with the (k-ω) model and shear stress transport (SST) to study the air profile inside a convective dryer. The model was utilized to modify the air distribution sieve to improve the air uniformity over the dryer width. The study was focused on the influence of the uniformity of air flow on moisture variability in the dryer. The model predictions were verified with on-field measured air velocity data from the plant dryer. The air distribution sieve, with an opening of 17%, significantly enhanced the downward velocity component and improved air flow uniformity by 64% compared to the base case.

5.3 Transient One-Dimensional

Chang et al. [59] proposed a numerical simulation and optimization for a multilayer belt dryer. They built a mathematical model depending on CFD techniques to study the simultaneous heat and mass transfer. The system of equations was solved using the finite difference method and programmed in C language. The model validation was compared with experimental data. The appropriate parameters for the structure and operating conditions of the dryer have been determined. When the belt velocity is 0.004 m/s, the conveyor flip time falls between 25 to 30 min. The belt length ranges from 6 to 7 m, and the multilayer belt dryer consists of 6 layers. The height of the air duct is between 0.2 to 0.3 m, and the material bed thickness is 10 cm. The air velocity ranges from 2.0 to 3.0 m/s. In summary, the drying kinetic data obtained from simulations were used to discuss and determine

the optimal parameters for the dryer structure and operating conditions. The parameters included the length of the belt for each layer, the height of the air channel between layers, and the number of belt layers. Additionally, the operating conditions discussed were the height of the material bed, belt velocity, and air velocity.

5.4 Transient Two-Dimensional

Alamia et al. [60] modelled the drying process of a belt dryer using two methods. The first one was a macroscopic heat and mass balances which describe the whole system. They were solved using the commercial process modelling software Aspen Plus V8.2 [61]. In the second method the authors created a 2-D transient CFD model using ANSYS Fluent 13.0 [56]. The necessary inputs of the macroscopic model, such as the temperature history of the biomass particles and the steam, as well as the change in particle moisture content over time, were obtained from the CFD simulations. Macroscopic modelling combined with CFD simulation, to propose a simple tool to estimate the dryer design. The macroscopic model was also verified experimentally to further improve its precision and reliability. The proposed CFD simulation setup can be utilized for optimizing the dryer design by considering three key aspects: bed height, steam injection temperatures, and fuel type.

Selimefendigil et al. [62] developed a numerical analysis for heat and mass transfer of a moving porous moist object in a two-dimensional channel, as a representation for a conveyor belt dryer. The process was simulated in 2-D laminar channel flow for different flow conditions by using the Finite Element method (FEM) with Arbitrary Lagrangian-Eulerian (ALE), using COMSOL Multiphysics [63]. The findings revealed that the heat transfer coefficient of the porous moist object in motion is not constant over time and varies locally. The study also highlighted the significant effects of increasing air temperature and velocity on the heat and mass transfer characteristics.

5.5 Transient Three-Dimensional

In 2017, Zhang et al. [64] used ANSYS Fluent [56] to study the impact of material thickness on a belt dryer's material moisture content and homogeneity as well as air velocity, temperature, and relative humidity. The results of their model were validated experimentally. In their model, they used Newton's second law, Eq. (20), to describe the change rate in the momentum. Also, they used porous medium and evaporation models and applied the mass and energy balance equations on an infinitesimal volume. Viscous dissipation was added to the energy equation using a User Define Function (UDF). In this function they used an empirical equation, Eq. (21), developed by Thorpe [65] for the source term in the energy equation together with a relationship developed by Hunter [66] for the adsorption heat on the surface of areca nuts and the latent heat of vaporization in free water, Eq. (22).

$$\frac{\partial\left(\rho_{\mathrm{a}} u\right)}{\partial t}+\nabla \cdot\left(\rho_{\mathrm{a}} u \vec{u}\right)=\nabla \cdot(\mu \cdot \operatorname{grad} u)-\frac{\partial \mathrm{p}}{\partial x}+s_u \tag{20}$$

$$S_h=-h_s(1-\beta) \rho s \frac{\partial W}{\partial t} \tag{21}$$

$$\frac{h_s}{h_v}=1+\frac{P_{sat}}{r}+\frac{dT}{dP_{sat}} \frac{dr}{dT} \tag{22}$$

where ρ_a is the fluid density in kg/m^3, u is the velocity in x-direction in m/s, t is the time in seconds, p is pressure on fluid infinitesimal volume in pascal, s_u is the source term, S_h are source item of energy equation, h_s stands for adsorption heat on areca-nut surface, β is porosity of areca-nut layer, W is the

moisture in areca-nut, h_v is the latent heat of vaporization in free water, T represents temperature and. r is the relative humidity of air.

In 2021, Zhang et al. [67] installed an auxiliary device in the drying chamber to modify how the air passages are organized. They used ANSYS Fluent [56] to figure out the best shape and angle of stacked feedstock. The modelling results were validated experimentally. The source terms were described and compiled as UDF by using the programming language C. The main findings indicated that a specific stacking method, known as vertical serration stacking with a 30° angle and a 43.0 mm interval, can enhance drying performance.

Çoban et al. [68] investigated the heat and mass transfer process of a conveyor belt dryer numerically using COMSOL 5.5 [63]. The authors used the study of Akpinar and Dincer [69] for convective drying of potato, to validate their study. A moving mesh path was used for providing the movement of the belt through the Arbitrary Lagrangian Eulerian (ALE) framework. The governing equations which describe the system were solved using the finite element discretization technique for the 3D transient problem. The results of the study highlighted the significant influence of varying parameters on the drying behaviour. Specifically, the impact of air velocity on evaporation was observed, with higher air velocities leading to increased evaporation rates. The most substantial reduction in moisture content, amounting to 63.12% loss, was achieved at an air velocity of 0.8 m/s.

Shen et al. [70] used COMSOL Multiphysics [63] to investigate the heat and mass transfer in microwave belt dryer, for germinated brown rice, numerically. They validated their model experimentally. The model describes the heat and mass transfer and the multi-physics fields including the transmission of microwave field. A discrete-combined approach was used as the strategy of the simulation to achieve the continuous movement of the samples in COMSOL using MATLAB [34] to create their three-dimensional model. The simulation improved understanding of heat and mass transfer processes. It showed that arranging magnetrons and adjusting microwave power could create a uniform electric field, aiding high energy absorption. Grain layer movement reduced energy absorption, leading to uniform temperature and moisture content distribution. Controlling microwave energy improved drying efficiency. Overall, the simulation offers insights for optimizing drying processes and controlling quality in materials like GBR.

Zhou et al. [71] used COMSOL Multiphysics [63] to simulate the heating process of a potato in a microwave conveyor belt dryer. They proposed a novel algorithm method using the implicit function and level set methods. The governing equations include the heat transfer process as well as electromagnetic field calculations. The moisture transfer was not considered in their simulation. The feasibility and accuracy of the methods were validated experimentally using temperature variations along the process. The proposed method demonstrated superior performance in calculating electric fields, scattering parameters, and power absorption curves. Validation results indicated that the method was more accurate and effective, with a five-fold increase in calculation efficiency compared to conventional methods.

Zhang et al. [72] investigated the berry slices' puffing properties under continuous microwave conditions in belt dryer using COMSOL Multiphysics software [63]. They used models of coupled multi-physics fields to study heat and mass transfer, as well as deformation of the slices. The model was validated experimentally. Results revealed insights into heat and mass transfer, deformation processes, and uniformity within the slices. The distribution of electric field profiles influenced microwave energy absorption and heat transfer, leading to volume expansion. Temperature, moisture content, and pressure exhibited local "hot spots" in the central region, stabilizing as the slice moved. Overall,

the study provides valuable guidance for optimizing technology parameters and controlling the puffing quality of berry slices.

Zhang et al. [73], in 2017, investigated the correlation between airflow velocity and feed thickness in a single-conveyor belt dryer using the (k-ε) standard turbulence model in ANSYS Fluent [56]. They used the 3D porous media formulation to model the process. They used experimental measurements to validate their model. In 2022, Zhang et al. [74] extended their research for four different fan frequencies using CFD simulation and experimental verification. Results showed that as feed thickness increased, airflow velocity became more uneven. At a feed thickness of 140 mm, airflow velocity was most even, ranging from 3.0 to 4.2 m/s. However, at higher thicknesses, such as 300 mm, the airflow velocity varied significantly, ranging from 2.4 to 6 m/s. The region of highest airflow velocity shifted from the outlet to the middle zone as feed thickness increased. The optimal feed thickness was found to be 140 mm due to the high airflow velocity near the outlet.

Ortiz-Jerez et al. [75] investigated a heat and mass transfer model to simulate the pumpkin slices drying process in RWD using COMSOL Multiphysics 4.3a [63]. They considered the impact of a typical plastic sheet's optical characteristics (Mylar®) on the radiative component of heat transfer. Equations for the conservation of mass and energy are developed that take into account the diffusion, capillary, and convective modes of movement. They performed the RWD drying experiment on thick slabs of pumpkin. The heat and mass transfer model were validated using two separate sets of experimental data for temperature and moisture. The results showed that there was only a 5% increase in the transmission of infrared (IR) radiation when a dry material was replaced by a wet material, challenging the notion of a "window" effect in RW drying as reported in the literature. For thin samples, the study found that moisture loss was sensitive to the temperature of water bath. The comparatively low temperatures detected in the samples were attributed to a substantial drop in the effective heat conductivity of food susbtance, which prevented the product temperature from approaching the water bath temperature. Conduction was identified as the primary mode of heat transfer to the material, with thermal radiation contributing only 1% of the total heat transfer.

Zhang et al. [76] used the finite volume method in ANSYS Fluent [56] to study the impact of conveyor positions on the distribution of airflow in three dryers. The CFD model used was the turbulent model for porous media with standard (k-ε). The three types of dryers (A, B and C), differ in their structure number of conveyors and feed thickness. The airflow through the dryer chambers was examined and illustrated using heatmaps based on the simulation findings. The following conclusions were drawn from the simulated results: Type C and type B dryers exhibited more uniform airflow distribution compared to type A dryer when the total feed thickness was the same. However, the use of four conveyors in types B and C led to higher production costs. Airflow velocity decreased when penetrating the feeds. The direction of airflow was from the left (inlet) to the right (outlet), with different airflow velocities observed on different conveyors due to their positions.

Table 4: Modelling results of CFD papers

Author	Dried product	Objectives	Results
Khankari et al. 1999 [54]		Illustrating the application of computational fluid dynamics (CFD) techniques for the simulation and analysis of a double-deck conveyor dryer. The authors aim to develop a numerical model that can predict variations in product moisture content and temperature and the corresponding impact on temperature and relative humidity of the drying air in the dryer.	The residence time depends on the drying agent temperature. At air temperature equals to 65°C residence time was 58 min. While by increasing the air temperature to 80°C the residence time was reduced to 38 min.
Böhner et al. 2013 [55]	Petroselinum crispum	Evaluating the inadequate air distribution in belt dryers, which leads to decreased throughput and high energy requirements using CFD simulations to identify issues with air distribution and propose modifications to optimize the airflow.	Results suggest that adjusting the angle of the air distribution flap and introducing additional air guiding plates improve the homogeneity of airflow and product moisture distribution in the drying process. The moisture content on both sides was similar at each belt by adjusting the flap setting to 45 degrees. It was in the range 65.4% to 74.1% wet basis at the end of the first belt and between 3.7% and 4.2% wet basis at the end of the fifth belt.
Zhang et al. 2020 [57]		Analysing the airflow distribution inside the dryer to provide insights for designing efficient belt dryers.	Airflow velocity across the feed layer ranged from 0.28 to 0.98 m/s, with a standard deviation of up to 0.17 m/s. Feed thickness and the size of the air space influenced airflow velocity. The most uniform airflow velocity at the feed surfaces was achieved with a feed thickness of 40 mm.
Mondal et al. 2022 [58]		Designing an optimized air distribution sieve for a single stage convective dryer using CFD simulation.	A 17% opening air distribution sieve boosted air flow uniformity by 64% over base case (without air distribution sieve) and optimized the downward velocity component.
Chang et al. 2013 [59]		Optimizing the dryer's structure and operating settings using numerical simulations and the establishment of a mathematical model for simultaneous heat and mass transport in a multilayer belt drier.	For optimal drying conditions, the belt velocity was set to be 0.004 m/s (25–30 min flip time of conveyor belt), length to 6–7 m, and layer count to 6. Keep the air duct 0.2–0.3 m above the 10 cm material bed and air velocity between 2.0–3.0 m/s. These conditions maximized efficiency and drying results while keeping energy costs in check.

(Continued)

Table 4 (continued)

Author	Dried product	Objectives	Results
Alamia et al. 2015 [60]	Biomass	Exploring the feasibility of high temperature drying for large-scale processes to maximize economic value.	A new biomass drying system using low-temp heat and built-in moisture recovery shows promise for efficient and sustainable gasification. It dries biomass to 1.95% moisture in 72 min, needing moderate heat and electricity. This system operates at 92.8% energy efficiency while its exergy efficiency is 52.9% outperforming traditional dryers. This is due in part to steam recovery and low-temp heat transfer.
Selimefendigil et al. 2021 [62]	Moving porous medium	Investigating heat and mass transport during convective drying of a moving porous medium in a two-dimensional rectangular channel with laminar flow conditions.	The study identified several key parameters that significantly influence the drying process: Air velocity: varying air velocities have a noticeable effect on evaporation. The reduction in moisture content for the lowest and highest air velocities ranged from 19.3% to 49.4% at the lowest air temperature and 44.8% to 85.7% at the highest air temperature. Air temperature: Higher air temperatures positively impact both heat and moisture transport.
Zhang et al. 2017 [64]	Areca-nut	Improving the internal air flow and moisture distribution in a belt dryer through numerical simulation and optimization.	Results showed that product thickness has the greatest impact on moisture content homogeneity, followed by velocity.
Zhang et al. 2022 [67]	Betel nut	Developing a simulation algorithm for dryers that incorporates complex flow channels, porous medium, heat and mass transfer, and complex feedstock geometries simultaneously to determine the optimal shape and angle of stacked feedstocks for uniform moisture distribution and efficient drying.	Results showed that that feedstock stacking with vertical serrations at a 30-degree angle and spaced 43.0 mm apart optimizes drying performance.
Çoban et al. 2021 [68]	Porous moist objects	Understanding the convective drying processes and investigate the heat and moisture transfer kinetics of moving porous moist objects to analyse the effects of varying parameters such as drying air velocity and temperature on their drying behaviour.	Results indicated a positive correlation between air velocity and evaporation, with the most substantial moisture reduction (63.12%) achieved at an air velocity of 0.8 m/s. Heat transfer differences between fixed and moving objects were minimal, averaging between 6% and 13%.

(Continued)

Table 4 (continued)

Author	Dried product	Objectives	Results
Shen et al. 2020 [70]	Germinated brown rice (GBR)	Understanding the complex continuous microwave drying process of GBR and analysing its drying characteristics.	Results revealed the effectiveness of microwave drying of GBR. Simulations closely matched real-world measurements, with temperature accuracy achieving an RMSE below 3.7°C and moisture content within 0.51%–1.37% (w.b.) across drying passes. The drying process maintained good uniformity, with temperature and moisture content uniformity coefficients ranging from 0.82–0.92 and 0.85–0.90, respectively.
Zhou et al. 2020 [71]	Potato slice	Developing a validated 3D numerical model that simulates microwave heating with continuous movement of food products on a conveyor belt utilizing the implicit function and level set methods.	The proposed method agreed well with experimental data with a maximum total absorption of around 195 W. The RRMSE between simulated and experimental temperatures were 2.47% and 3.16% for the proposed and traditional methods, respectively.
Zhang et al. 2022 [72]	Berry slice	Investigating the heat and mass transfer and the deformation process of berry slices during microwave puffing to understand the distribution of electric field profiles, moisture content, temperature variations, and volume deformation of the berry slices.	Simulated and measured data showcased similar trends. Temperature rose quickly from 20°C to 87°C initially, with an average difference between simulation and experiment of 4.78°C. Moisture content decreased swiftly from 30% to 27.54%, with an average simulated-measured difference below 1.21%. Internal pressure peaked at 750 mm (8.42 × 105 Pa, close to the theoretical value) and then steadily declined due to deformation and increased gas permeability. Volume expansion followed pressure, rapidly inflating from 750 to 1500 mm and then stabilizing later.
Zhang et al. 2017 [73]		Evaluating the impact of feed thickness on the airflow velocity distribution and provide recommendations for an optimal feed thickness setting.	Results indicated that thicker feed (140–300 mm) exhibited wider velocity variations and shifted the high-velocity zone towards the chamber centre. Variance increased with thickness, likely due to reduced space between feed and air inlet. An optimal feed thickness of 140 mm was recommended for consistent and high airflow near the outlet, crucial for efficient drying.

(Continued)

Table 4 (continued)

Author	Dried product	Objectives	Results
Ortiz-Jerez et al. 2015 [75]	Pumpkin slices	Developing a model-based mechanistic understanding of the drying process through Refractance Window^{TM} drying to explore the impact of Mylar$^{®}$'s optical properties on the radiative component of heat transfer during pumpkin slices drying.	The transmission of infrared radiation through the Mylar sheet increases by only 5% between a dry and wet product. A major portion (99%) of thermal energy is transferred through conduction rather than radiation.
Zhang et al. 2017 [76]		Simulating airflow distribution in three types of belt dryers with different conveyor positions using CFD to identify optimal dryer design.	The simulations reveal that Type B and C dryers provide more even airflow throughout the feed compared to Type A at the same depth but incur higher costs due to their four conveyors. Airflow slows as it penetrates the feed, and travels consistently from left (inlet) to right (outlet). Quantitative results confirmed the left-to-right flow direction, with higher velocities on the right side (1.05–1.32 m/s) compared to the left side (2.89–0.87 m/s).

6 Empirical

This section presents an overview of the empirical modelling techniques presented in the literature. The results of these studies are summarized in Table 5.

Soodmand-Moghaddam et al. [77] performed drying experiments, at three levels of air velocity and three levels of drying temperature, to dry lemon verbena. They used a continuous flow dryer with solar-powered pre-heating system. The authors compared ten different mathematical models, to both older [16,78–80] and newer [17,81–84] models published after 2000 as well as the most established correlation: to their experimental results [15]. Different regression models were performed using MATLAB [34] and SPSS 11.5.1 software package [85]. The highest matching model was the Midilli and Kucuk's model [15]. A summary of most relevant final moisture content correlation is found in Table 6.

Soodmand-Moghaddam et al. [86] investigated the fuel consumption and the drying characteristics of lemon verbena leaves in a continuous dryer. They prepared an experimental model using 4 conveyor belts. Experiments were conducted at three drying air temperature levels and three air velocity levels. The drying system worked by two working conditions, solar gas drying (SGD) and gas drying (GD). The central composite design-Face Cantered technique with response surface methodology was used for the optimization of the drying process. The optimized drying conditions for lemon verbena leaves were achieved at a drying temperature of 39.54°C and an air velocity of 2 m/s. Under these conditions, no fuel was consumed, the drying time was 131.48 min, and the essential oil (EO) content was 0.52%.

Chayjan et al. [87] prepared an experimental setup for the conveyor belt dryer, used for drying fresh samples of the terebinth fruit. The experiments were performed to study the effect of different drying conditions, specifically air temperature and velocity, on the thermal and physical properties of the terebinth fruit, namely effective moisture diffusivity, activation energy, changes in shrinkage, colour, and mechanical properties. The experiment was done with five replicates. The authors compared six

different mathematical models, older models [18], and newer models [15,83,88,89] published after 2000, that can describe the moisture content at various stages of drying, to their experimental results. Using the curve expert software [90], they found that the highest matching model was the Midilli empirical model [15].

Jafarifar et al. [91] prepared an experimental setup for drying walnut kernel. The experiments were performed to study the effect of various drying techniques on the thermal and physical properties of the walnut kernel, namely shrinkage, colour changes, activation energy and effective diffusivity. The experimental results were collected under various drying conditions, namely air temperature and velocity, and fitted with 10 different thin layer drying models' moisture ratios, older models [16,18,78,80], and newer models [82,89,92–94] published after 2000 as well as the most established correlation: [15]. The selection of the best model was done through three criteria: R^2, X^2 and RMSE. Midilli model [15] resulted in best performance amongst all three technologies.

Montazer-Rahmati et al. [95] designed and constructed a bench-scale semi-continuous convective dryer for picrate drying. The moisture contents both final and equilibrium, at various air temperatures and air velocities, were experimentally evaluated using the Karl-Fischer test [96]. The experimental crude data were processed to calculate the moisture ratio, the drying flux, the moisture diffusivity, and the internal and external mass transfer coefficients. The curves were then plotted and fitted using the Table Curve software in Microsoft Excel [97]. To relate the model parameters to the drying conditions, a stepwise multi-linear and nonlinear regression analysis based on the Levenberg-Marquardt (L-M) algorithm. The exponential-hyperbolic decay model was the best describing model to predict the moisture ratio of picrate. Internal mass transfer coefficient empirical correlation was modelled as function of moisture content and presented in Table 7.

Yang et al. [98] developed a small-scale infrared belt dryer for rapeseed. To investigate the drying performance, they fitted the experimental data obtained to five commonly thin-layer drying models [16,78,83,84,99]. The two-term model [84], followed by Page model [78], provided the best fit to the experimental results. The effective moisture diffusivity was calculated by graphing experimental drying data *vs*. the drying time and the natural logarithm of MR.

Ostrikov et al. [100] proposed an empirical-mathematical modelling approach to explore the drying kinetics of cereals with a fluctuating heat supply using the stitched method. The proposed technique is based on assembling drying curves together. Control variables such as the specific load of grain, the air temperature, velocity, and humidity at the entrance into the drying layer, and other control variables were assumed to be piecewise constant functions. As such, the drying process was separated into discrete time regions. All calculations were investigated in a specially designed software program to perform the calculation of the drying process with respect to changes in air humidity. The modelling method was validated experimentally. A software-based algorithm for controlling the drying process under variable heat supply was developed, leading to the design of a grain dryer that can adjust the grain layer height from compartment to compartment. This design facilitates uniform drying and minimal energy consumption.

Ogunnaike et al. [101] used a continuous flow belt dryer to investigate the influence of the drying variables on the fish feed drying kinetics. The experimental data were obtained under various drying conditions, particularly air temperature and velocity and belt velocity. To select the most accurate model describing the drying process, the experimental data results were collected and fitted, using the non-linear regression approach on Microsoft Excel, to seven empirical models, older models [78–80] and newer models [15,81,84,99] published after 2000. The most accurate model was given by Midilli et al. [15].

Liu et al. [102] performed a mathematical model for panax notoginseng drying in a vacuum belt dryer. An experimental set up was developed to investigate the impact of the drying parameters as temperature, feeding speed and belt speed on the drying rate. Experiments were conducted under different conditions then five mathematical models [16,18,78,80,83] were fitted to the drying curves to evaluate the most accurate model. The logarithmic model [83] was the best-fit one to predict the drying process.

Fumagalli et al. [103] developed a pilot-scale belt dryer to analyse the drying of brachiaria brizantha seeds in different dryer modes at different temperatures and velocities. The equipment developed could operate in different modes such as fixed-or fluidizied-bed mode, or conveyor belt mode, providing homogeneous drying. The experimental data of moisture content variations along the dryer was plotted *vs*. the drying time. The resulted curves were fitted to a one-term exponential model [104] to obtain the correlation coefficients. Results showed that inlet air velocity variations had no significant effect on drying kinetics. Drying kinetics were similar in fixed, conveyor belt, and fluidized bed modes at the same temperature. Drying in a fluidized bed mode yielded better germination potential. A drying temperature of 50°C and storage moisture content below 10% were recommended for maintaining physiological quality. The proposed approach was advantageous over traditional conveyor belt drying, requiring a shorter belt length for the same moisture reduction.

Xu et al. [105] used a continuous vacuum dryer to investigate the kinetics of removing moisture from tortilla chips. The experiments were conducted at three conduction plate temperatures and three product thicknesses. Four empirical models [2,16,78,105] were applied to fit the experimental data, to study the influence of drying thickness and temperature on the drying rate. The authors observed that the variable drying coefficient model [105] and the Page model [82] perfectly match the experimental data.

Jafari et al. [106] fabricated a semi-industrial continuous microwave dryer to investigate the energetic and exergetic performance of the dryer and observe the qualitative changes of the crop during drying. The experiments were carried out at different thickness of the product, different product feed velocity and microwave power. The experimental results were fitted with five empirical and semi-empirical models [16,18,78,80,84] to choose the appropriate model. The Wang et al. model [80] and the Page model [78] were found to be the best models for a thickness of 6 mm at powers of 90 and 450 W, and a thickness of 6 mm at power of 270 W, respectively. On the other hand, the Lewis model [18] and the two-term model [84] were found to be the best models for a thickness of 12 mm at powers of 270 and 450 W, and a thickness of 12 mm at power of 90 W, respectively.

Zareiforoush et al. [107] tested and refined the performance of a solar-assisted multi-belt dryer. To study the effect of thermal energy sources on stevia leaf drying, an experimental setup was constructed using solar-gas water heaters and solar-powered infrared (IR) lamps. The experiment examined how drying air velocity, temperature, and IR lamp power affected the drying process. To improve the drying system, a Response Surface Methodology (RSM) analysis was performed, concentrating on performance factors. Two operational modes were identified: a hybrid mode and a solar-assisted mode. The study analysed Overall Specific Energy (OSE), Non-Solar Specific Energy (NSE), Overall Energy Efficiency (OEE), and Solar-Assisted Energy Efficiency (SEE) of a drying system. The lowest OSE (17.30 MJ/kg water evaporated) was achieved at 7 m/s air speed and 40°C without IR power. The lowest NSE (2.71 MJ/kg) was at 7 m/s, 40°C and 300 W. Maximum OEE (13.92%) and SEE (88.71%) were at 7 m/s and 40°C with 300 W IR power for SEE and none for OEE. RSM identified the optimum conditions as 7 m/s, 39.96°C and 300 W, with drying time of 180.95 min, NSE of 1.062 MJ/kg, and SEE of 84.63%.

Table 5: Modelling results of empirical papers

Author	Dried product	Objectives	Results	Validation method or verification approach
Soodmand-Moghaddam 2020 [77]	Lemon verbena leaves	Developing a mathematical model for lemon verbena leaves drying in a continuous flow dryer equipped with a solar pre-heating system.	The results indicate that the drying temperature and air velocity significantly influenced the drying time. The highest essential oil content in the dried lemon verbena leaves was observed at a temperature of 40°C and an air velocity of 1 m/s. The suitability of 10 different mathematical drying models was evaluated, and it was found that the Midilli and Kucuk's model successfully predicted the experimental data in all tested conditions.	The validation of the drying model for lemon verbena leaves involved comparing its predictions to experimental data obtained at varying temperatures (50°C, 40°C, 30°C) and air velocities (2, 1.5, 1 m/s). Among 10 tested models, the Midilli and Kucuk model showed the best performance, with R^2 values above 0.999 and RMSE and χ^2 values below 0.0174 and 0.0019, respectively. These results demonstrate the model's high accuracy in predicting drying kinetics under all tested conditions.
Soodmand-Moghaddam et al. 2019 [86]	Lemon verbena leaves	Investigating fuel consumption and drying characteristics of lemon verbena leaves in a continuous flow dryer equipped with a solar pre-heating system to minimize the use of fossil fuels and optimize the drying conditions to achieve the desired essential oil content.	The solar gas drying mode resulted in zero fuel consumption at drying temperatures of 30°C and 40°C for any air velocity. In contrast, gas drying mode fuel consumption increased with higher inlet air temperatures. The optimal drying conditions of lemon verbena leaves were determined at drying temperature of 39.54°C and an air velocity of 2 m/s. The drying time under these conditions was 131.48 min. The essential oil content of lemon verbena leaves varied with different drying conditions. The highest content of 0.60% was obtained at 40°C and 2 m/s, while the lowest content of 0.33% was obtained at 50°C and 1 m/s.	The validation of the drying model for lemon verbena leaves was conducted using experimental data from a continuous flow dryer with solar pre-heating, tested at temperatures of 30°C, 40°C, and 50°C and air velocities of 1, 1.5, and 2 m/s. Using the central composite design and response surface methodology, the model accurately predicted drying time, essential oil content (EO), and fuel consumption. The model's accuracy in predicting the outcomes confirms its reliability for optimizing drying processes.

(Continued)

Table 5 (continued)

Author	Dried product	Objectives	Results	Validation method or verification approach
Chayjan et al. 2016 [87]	Terebinth fruit	Analysing and modelling continuous drying characteristics of terebinth fruit.	Experiments calculation revealed the following for terebinth fruit: The effective moisture varied between 6.48×10^{-11} and 2.34×10^{-10} m^2/s. The activation energy for moisture diffusion and evaporation was between 25.45 and 35.16 kJ/mol. Specific energy consumption ranged from 10.5 to 65.2 GJ/kg. The maximum shrinkage value observed was 16.70% at an air temperature of 75°C and the minimum shrinkage value was 12.34% at an air temperature of 45°C. Total colour difference increased, while the hue angle and chroma decreased. The rupture force for dried terebinth fruit samples ranged from 80.15 to 112.68 N mm.	The study validated six mathematical models to predict terebinth fruit drying kinetics by fitting experimental data to each model using non-linear regression analysis. Validation was assessed using statistical metrics: coefficient of determination (R^2), reduced chi-square (v^2), and root mean square error (RMSE). The Midilli model was identified as the most suitable due to its high R^2 and low v^2 and RMSE values, demonstrating its superior accuracy in representing the experimental drying behavior. The experiments were conducted using a semi-industrial continuous belt dryer with three floors. Each floor was equipped with adjustable centrifugal blowers for air velocity control and industrial heating elements regulated by a thermostat to maintain specific temperatures. An insulated air channel ensured even heat distribution, while a PVC conveyor belt with an adjustable speed motor transported the product. Additional heating was provided by infrared lamps, and instruments such as thermometers and humidity meters monitored conditions. Steady-state operation was achieved before experiments, which were conducted at varying air temperatures (45°C–75°C), air velocities (1–2 m/s), and belt speeds (2.5–10.5 mm/s).
Jafarifar et al. 2017 [91]	Fresh walnut	Modelling the physical and thermal properties of walnut kernels during drying processes employing microwave semi-industrial continuous drying (M-CD), microwave infrared-vacuum drying (M-IVD), and microwave infrared-fluidized bed drying.	The M-CD dryer, operating at a microwave power of 270 W, air temperature of 45°C, and belt linear speed of 10.5 mm/s, achieved the lowest shrinkage (6.53%) and colour change (5.54%). Conversely, the M-IVD dryer, utilizing a microwave power of 630 W, drying temperature of 75°C, and absolute pressure of 60 kPa, resulted in the highest shrinkage (14.65%) and colour change (18.28%). The lowest and highest values of effective moisture diffusivity (1.04×10^{-8} and 9.74×10^{-8} m^2/s, respectively) were observed in the M-CD method. The M-CD method was considered the most suitable technique for walnut kernel drying as it produced dried samples that were most similar to fresh ones.	The study validated ten mathematical models to describe the drying behavior of walnut kernels by fitting experimental data to each model and evaluating their accuracy using statistical metrics: coefficient of determination (R^2), reduced chi-square (χ^2), and root mean square error (RMSE). The experiment involved studying the drying behavior of walnut kernels using three distinct drying technologies: microwave semi-industrial continuous drying (M-CD), microwave infrared-vacuum drying (M-IVD), and microwave infrared-fluidized bed drying (M-IFD). Experimental data were collected under varying drying conditions, including air temperature, microwave power, belt speed, pressure, and infrared radiation.

(Continued)

Table 5 (continued)

Author	Dried product	Objectives	Results	Validation method or verification approach
Montazer-Rahmati et al. 2005 [95]	Rapeseed	Investigating the drying kinetics and behaviour of picrite and to establish optimal drying parameters.	The exponential-hyperbolic decay model is highly recommended for predicting the drying curve behaviour of picrite at a temperature range of 40°C–100°C. Fan frequency has a significant effect on the drying time. As the fan frequency was 25, 30, 35, and 40 Hz, the time to reach the moisture content less than 10% was about 30, 30, 25, and 20 min, respectively.	The study validated a theoretical model for predicting the drying kinetics of picrite by comparing its predictions with experimental data, statistical evaluations, and results from related studies. Experimental data on picrite drying was collected using a thin-layer drying method, and the model's predictions were compared against these observations. The experiments were conducted using a bench-scale semi-continuous convective dryer equipped with instruments to monitor drying conditions, including a blower, desiccator, hygrometer, orifice meter, heating duct, drying duct, and psychrometer. A total of 24 experiments were performed at varying temperatures (40°C, 60°C, 80°C, and 100°C) and air velocities (0.5 and 1.5 m/s), with equilibrium moisture content also measured. The experimental data not only validated the theoretical model but also provided the basis for designing a conveyor-belt dryer tailored for picrite. The study concluded that the model could accurately predict drying kinetics and serve as a reliable tool for dryer design.
Yang et al. 2017 [98]	Rapeseed	Studying the influence of process parameters on drying performance, fitting experimental data to thin-layer drying models, and calculating the effective moisture diffusivity of rapeseeds.	The exponential-hyperbolic decay model accurately predicts how picrite dries between 40°C and 100°C, outperforming other tested models. The empirical model effectively captures how moisture travels inside picrite during drying, considering moisture content, air temperature, and air velocity. The Ackermann correction factor and flowing air temperature significantly impact drying efficiency in picrite and must be included in accurate analysis and modelling.	The study validated five thin-layer drying models to predict rapeseed drying behavior during infrared drying by fitting experimental data under varying conditions, including temperature, radiation distance, initial moisture content, and layer thickness. Statistical metrics like R^2, χ^2, and RMSE were used to evaluate model accuracy, with the Two-term model proving most suitable, followed by the Page model. Experiments were conducted using a small-scale infrared belt dryer equipped with adjustable infrared heaters, a conveyor system, ventilation fans, and a precise control module. Rapeseed samples, rehydrated to specific moisture contents, were tested under conditions designed using the Taguchi methodology to assess drying performance. This controlled experimental setup ensured reliable data, confirming the Two-term model's accuracy in predicting rapeseed drying kinetics.

(Continued)

Table 5 (continued)

Author	Dried product	Objectives	Results	Validation method or verification approach
Ostrikov et al. 2021 [100]	Barley grain	Developing an empirical-mathematical modelling for investigating the drying kinetics of cereals under variable heat supply using the stitched method.	The developed empirical-mathematical model outperformed existing methods with a maximum absolute deviation of only 13% compared to actual drying data. Compared to other methods, this approach allows for dry mode optimization and better accounts for thermal-humidity constraints. The proposed model can be applied to various cereal crops beyond the tested barley, requiring only experimental drying curves and specific empirical dependences for each crop.	The study validated the mathematical model by comparing its predictions to experimental data. The experiments simulated barley grain drying under variable heat supply, with controlled parameters including drying temperature, heated air velocity, air humidity, and the specific load of grain on the gas distribution grid. These parameters were adjusted in stages to mimic real-world drying conditions. Measurements of grain moisture content, temperature, and air humidity were collected throughout the process and used to validate the model. Additionally, a software program was developed to predict optimal drying conditions, enabling more efficient drying processes that conserve energy and maintain grain quality.
Ogunnaike et al. 2021 [101]	Extruded fish feeds	Modelling the kinetics of drying extruded fish feeds in a continuous belt dryer to investigate the influence of drying variables, such as air temperature and velocity on the drying kinetics of the fish feed.	Higher drying temperatures (60°C to 100°C) led to significantly faster moisture loss compared to lower temperatures, confirming that elevated temperatures promote rapid evaporation of surface moisture in the extrudates. Seven existing mathematical models were compared to fit the drying data using non-linear regression, Midilli et al.'s model yielded the best overall goodness-of-fit parameters across various air temperatures and conveyor belt speeds (50 m/s). Specifically, R^2 ranged from 0.9923 to 0.9995, indicating excellent agreement between predicted and experimental moisture ratios.	The study validated seven thin-layer drying models for extruded fish feeds under varying drying air temperatures (60°C–100°C) and velocities (0.7–0.9 m/s), using statistical metrics like R^2, χ^2, SEE, SSE, and RMSE. The Midilli et al. proved the most accurate. Experiments were conducted in a controlled setup using a continuous flow belt dryer at a constant belt speed of 50 m/s, drying 2000 g of fish feed until weight stabilization. This comprehensive approach confirmed the Midilli et al. model's effectiveness in predicting drying behavior and optimizing the process.
Liu et al. 2009 [102]	*Panax notoginseng*	Developing a mathematical model for the vacuum belt drying (VBD) process of *Panax notoginseng* extract and examining the impact of drying temperature, feeding speed, and belt speed on the drying rate.	Various mathematical models (Lewis, Page, Henderson, and Pabis, Logarithmic, Wang and Singh models) were tested and compared to describe the VBD process. The Logarithmic model provided better predictions compared to other models and satisfactorily described the VBD process. The effective moisture diffusivity of *Panax notoginseng* extract ranged between 4.86×10^{-7} and 11.0×10^{-7} m^2/s under the different drying conditions.	The study validated its mathematical models by comparing their predictions to experimental data on the drying kinetics of *Panax notoginseng* extract. A laboratory-scale vacuum belt dryer was used. The *Panax notoginseng* extract was spread in a thin layer on a conveyor belt that moved through the dryer. The dryer had two heating zones and a cooling zone. The researchers tested different combinations of drying temperatures (90°C, 100°C, and 110°C), feeding speeds (how fast the extract was added to the belt), and belt speeds. They measured the moisture content of the extract at different points along the belt to see how it changed over time.

(Continued)

Table 5 (continued)

Author	Dried product	Objectives	Results	Validation method or verification approach
Fumagalli and Freire 2007 [103]	*Brachiaria brizantha*	Studying the drying kinetics of *B. brizantha* grass seeds using a pilot-scale belt dryer that operates as either a fixed bed or fluidized bed to develop a drying process that ensures the stability and long-term storage of the seeds while maintaining their physiological quality.	The study found that air velocity had little impact on drying rate, which was mainly controlled by temperature and moisture content. Three mathematical models accurately predicted the drying data, and higher temperatures led to faster drying but slightly lower physiological quality for the seeds. While the belt conveyor alone was insufficient to reach the ideal moisture level, a combined process using all three drying methods could achieve this efficiently. Optimally, seeds could be dried for 180 min at 30°C or 45 min at 50°C, with higher temperatures potentially requiring a dormancy overcoming process before planting to maximize germination.	The study validated its mathematical model by comparing its predictions to experimental data on the drying kinetics of *Brachiaria brizantha* grass seeds. The accuracy of the model was evaluated using statistical measures like the correlation coefficient (R), reduced chi-square (v^2), mean bias error (MBE), and root mean square error (RMSE). The model demonstrated a good fit to the experimental data, indicating that it could accurately predict the drying behavior of the seeds.
Xu et al. 2012 [105]	Low-fat tortilla chips	Developing drying models and understand the effects of drying thickness/temperature on the drying rate of low-fat tortilla chips using a continuous vacuum drying method and predicting appropriate drying times, optimizing process conditions, and gaining a better understanding of the drying mechanisms.	Drying rates were evaluated at conduction plate temperatures of 80°C, 90°C, and 100°C and product thicknesses of 0.8, 1.5, and 2.3 mm. The drying data were fitted using an effective diffusion model and semi-empirical models. All models showed good agreement with the experimental data, with $R^2 > 0.98$. The Page and variable coefficient models provided the best fit to the experimental data, considering other goodness-of-fit indicators such as the sum of squared errors (SSE) and chi-squared error with values of 0.00348 and 9.41×10^{-5} for Page model at 100°C plate temperature and 0.0506 and 6.03×10^{-5} for variable coefficient model.	The validation of the drying models in the study was conducted through a comparative analysis of experimental and predicted moisture content data for low-fat tortilla chips under controlled vacuum drying conditions. Experimental data were collected at conduction plate temperatures of 80°C, 90°C, and 100°C and product thicknesses of 0.8, 1.5, and 2.3 mm. The study tested multiple drying models, including diffusion, semi-empirical (Henderson-Pabis and Page), and a variable drying coefficient model. The models' performance was evaluated using goodness-of-fit metrics as mentioned in the results section.
Jafari et al. 2017 [106]	Rice grains	Performing energy and exergy analyses of a semi-industrial continuous microwave dryer to study the qualitative changes in the crop during the drying process.	The study revealed that most microwave energy absorption occurred near the grain's penetration depth (1–1.5 times its diameter), leading to higher temperatures and improved moisture reduction. Increasing the paddy layer thickness boosted energy and exergy efficiencies at fixed power, while higher power within the same layer reduced these efficiencies. Ultimately, the best drying performance was achieved with a layer thickness of 18 mm and a power of 90 W, minimizing energy consumption, maximizing efficiency, and minimizing grain breakage.	The validation process involved a detailed comparison of the empirical model's predictions against the experimental data obtained from the specifically designed continuous band microwave dryer. This comparison focused on key drying parameters like moisture ratio, effective moisture diffusivity, and energy efficiency. The experimental setup was carefully designed to provide accurate and reliable data for this validation process.

(Continued)

Table 5 (continued)

Author	Dried product	Objectives	Results	Validation method or verification approach
Zareiforoush et al. 2022 [107]	Stevia leaves	Evaluating and optimizing the performance of a solar-assisted multi-belt conveyor dryer using response surface methodology.	The lowest overall specific energy value obtained was 17.30 MJ/kg of water evaporated with a drying air speed of 7 m/s and a temperature of 40°C, without using infrared (IR) power. The lowest non-solar specific energy value achieved was 2.71 MJ/kg of water evaporated with 7 m/s drying air speed, 40°C temperature, and 300 W IR power. The maximum overall energy efficiency was 13.92%, while the maximum solar-assisted energy efficiency was 88.71%. The difference between them was the application of 300 W IR power for maximum solar assisted technology. The optimum operating conditions according to the response surface methodology, were a drying air speed of 7 m/s, a temperature of 39.96°C, and 300 W IR power. Under these conditions, the drying time was 180.95 min, with a non-solar specific energy of 1.062 MJ/kg of water evaporated, and the solar-assisted energy efficiency was 84.63%.	The paper primarily focuses on the design, performance analysis, and optimization of the solar-assisted multi-belt conveyor dryer using experimental data and Response Surface Methodology (RSM). The results provided, such as energy efficiency and drying time under various conditions, are based on the experimental setup, but there is no direct validation with other established systems or theoretical models. While the experimental findings support the effectiveness of the solar-assisted drying system, the study doesn't explicitly compare or validate its results against other models or real-world systems, which is a typical aspect of a validation process.

7 Control Methods

The literature review shows that several researchers have conducted studies on the performance behavior of belt dryers using various control systems. Classic control systems were employed in several studies [108–112] to evaluate the performance of belt dryers for processes like drying mate leaves, grains, and raisins. These systems typically utilized PI and PID controllers in feedback loops to regulate parameters such as moisture content, air temperature, and belt speed, relying on real-time measurements and predefined setpoints. In some cases, cascade configurations were employed for enhanced disturbance rejection. While effective, these controllers faced challenges with complex nonlinear drying dynamics, such as sensor delays and parameter uncertainties, which were addressed through strategies like feedforward compensation, adaptive tuning, and numerical optimization. Johansen Van Delft [113] used the model predictive control, A detailed dynamic model of the conveyor belt dryer, incorporating relevant physical and chemical phenomena, was developed and verified. This model provides the foundation for MPC, which anticipates future conditions by predicting drying behavior. By optimizing control actions over a set prediction horizon, MPC ensures efficient operation and maintains product quality, especially in complex multivariable control scenarios with constraints. While in recent years, Artificial Intelligence (AI) techniques, such as Artificial Neural Networks (ANNs) and Adaptive Neuro-Fuzzy Inference Systems (ANFIS), have gained attention as advanced control systems [114–117]. These controllers can handle the nonlinearities and uncertainties of the drying process more effectively than traditional methods.

• ANNs are implemented by training the network with old data to predict drying outcomes. Once trained, ANNs can adjust operational parameters like temperature and belt speed dynamically to

achieve optimal drying conditions. The optimization of ANN-based controllers involves tuning the network structure and learning parameters to balance accuracy and computational efficiency.

• ANFIS combines the adaptability of neural networks with the interpretability of fuzzy logic, utilizing fuzzy if-then rules to guide control actions. ANFIS models are optimized through hybrid learning, which adjusts the fuzzy membership functions and rules for accurate and adaptive control. This hybrid approach allows ANFIS to maintain effective control in response to varying drying conditions.

Finally, Jensen et al. [51] presented an empirical software-sensor model, which uses data-driven methods to estimate drying parameters indirectly. This approach allows for real-time monitoring and control without requiring physical sensors for every variable, which can be beneficial in reducing costs and complexity. The results of these investigations are presented in Table 8.

7.1 Classic Control

Kiranoudis et al. [108] investigated the dynamic behaviour of the drying process by belt dryer. For this aim, they made a mathematical model composed of algebraic equations as well as ODEs. The algebraic equations were solved through a Newton-like method employing a Broyden-type approximation for the calculation of the system's Jacobian matrix. While the ODEs were calculated for each step using Simpson's method of numerical integration. The proposed procedure yielded a transfer function of the second order as shown in Eq. (23). To achieve excellent control of material moisture content at the exit of each chamber in the dryer, a PI-feedback cascade temperature controller was employed, assuming instant measurement of the input material moisture content.

$$\delta X_s = \begin{bmatrix} \dfrac{0.243}{0.95s+1} & \dfrac{1.226e^{-0.59s}}{(0.58s+1)(1.79s+1)} \end{bmatrix} \begin{bmatrix} -\delta T_{AC} \\ \delta X_{sO} \end{bmatrix} \tag{23}$$

While X_s is material moisture content of product stream on leaving the chamber, T_{AC} is the temperature of drying air stream and X_{sO} is the initial material moisture content.

Dai et al. [109] constructed a genetically optimized fuzzy immune PID controller (GOFIP) for the drying process of a conveyor belt dryer. This controller operates by both intelligent fuzzy immune feedback control and traditional control. Then they simulated two other controllers, the general PID controller and the fuzzy PID controller. The three controllers were compared with an experimental model. The GOFIP controller was found to be superior compared to the other two simulated controllers.

Tussolini et al. [110] experimentally evaluated a feedback strategy for the control of drying mate leaves in a conveyor belt dryer. A dynamic drying model, consisting of two partial differential equations representing energy and mass balances within the solid phase of the dryer, was employed. PID controller parameters and manipulated conveyor velocities were calculated using this model under conditions identical to the experimental setup. The dynamic 1-D drying model was solved using the numerical method of lines by applying a backward differentiation formula to the first-order time and space derivatives.

Mansor et al. [111] developed Quantitative Feedback Theory (QFT) based self-tuning controller for drying grain plants in the conveyor belt dryer. On the basis of real-time input/output data, system identification was used to develop a mathematical model of the grain dryer. An experimental setup has been built, collecting its input and output data to be used in the mathematical model. Moreover, the MATLAB System Identification Toolbox (MSIT) [34] was used to simplify the calculations into a linear process to be used in the QFT technique. Prediction Error Minimization (PEM) was used to

estimate the model parameters. QFT-based self-tuning controller demonstrated superior performance in tracking reference signals, attenuating disturbances, and adapting to parameter variations compared to the standard QFT-based controller.

Zanoelo et al. [112] proposed a semi empirical model to reproduce the kinetics of drying mate leaves under transient conditions in a continuous shallow packed bed drier. They investigated a model for transient drying and the mathematical procedure to solve it, the numerical method of lines approximates the first order spatial and time derivative using a backward differentiation formula (BDF). The subsequent step was designing the control system. Using this reliable model, a control strategy was proposed to maintain an acceptable discharge moisture content by manipulating the velocity of conveyor belt to account for variations in operating conditions. The performance of a PID and PI controller was evaluated by comparing the open- and closed-loop responses of discharge moisture content to random variations in the discharge moisture content, drying temperature, and air velocity. The PI controller was found suitable for controlling moisture content in conveyor-belt dryers of mate leaves, with the derivative action of the PID controller deemed insignificant. Time variations in feed moisture content, drying temperature, and air velocity were considered key factors affecting the process.

7.2 Advanced Control

Johansen Van Delft [113] developed a predictive control model for a conveyor belt dryer. His mathematical model was composed of a system of PDEs that were simplified using a finite difference approximation. These equations were further simplified and linearized to form a set of ODEs to be used in model-based control solution. Heat and mass transfer were described in Eqs. (24), (25). The ODEs system was solved by MATLAB ode23tb function [34]. Further, by balanced residuals, the model was reduced to fit Model Predictive Control (MPC).

$$\delta_U = hv\left(T_g - T_p\right) \tag{24}$$

$$\delta_M = \frac{hv}{\lambda_0}\left(T_{dp}(\gamma) - T_g\right)\zeta(\alpha) \tag{25}$$

where δ_U and δ_M are the heat transfer and drying rate, respectively. h is the heat transfer coefficient, while v is the evaporation area/volume product ratio. λ_0 is the latent heat of water. T_g, and T_p are the gas mixture and product temperature, respectively. $\zeta\ (\alpha)$ is the falling rate multiplicator of drying rate.

Bakhshipour et al. [114] proposed two methods for modelling of drying stevia leaves in an infrared-assisted continuous hybrid solar dryer. In the first method, they used mathematical modelling. MATLAB's curve fitting toolbox [34] was used to determine the constants of the evaluated models. They found that the Midilli et al. [15] model provided the best results in 24 conditions. In the second method, they used intelligent modelling methods such as Artificial Neural Networks (ANN) and Adaptive Network-based Fuzzy Inference System (ANFIS). Both models were developed with different structures to predict the MR data. Both models were compared to the experimental data using 3 criteria: R^2, X^2 and RMSE. The ANN model was the most precise and had the best performance statistics.

Lutfy et al. [115] developed a reliable conveyor belt dryer model using system identification techniques based on ANFIS modelling capabilities. They built a laboratory-scale conveyor belt grain dryer to compare the experimental MR results with the ANFIS model. Moreover, a comparative study was made by other models to determine the effectiveness of the proposed model. The other models used were the Auto Regressive with Xogenous input (ARX) and ANN. The modelling performance

was evaluated using the RMSE criterion. The comparative study with the three models showed the superiority of the ANFIS model over the other two models.

Lutfy et al. [116] later modified their previous ANFIS model [115] to deal with the dehydration process' inherent complexity and nonlinearity. Specifically, a laboratory-scale conveyor belt grain dryer for rough rice was designed and built. The system identification technique was applied to the experimental data, collected from the dryer, for the development of the ANFIS model. MATLAB "anfis" function [34] was used to employ this hybrid training technique for the initial ANFIS structure. A simplified PID-like ANFIS controller is used as a main controller to control the drying process. RMSE was utilized to evaluate the performance of the ANFIS modelling system. A comparative study has demonstrated that the PID-like ANFIS controller is superior to a genetically tuned conventional PID controller for controlling the grain drying process.

Lutfy et al. [117] then introduced type 2 fuzzy sets to cope with the uncertainties that can exist in the fuzzy system's rule basis. They employed a Nonlinear AutoRegressive with eXogenous input (NARX) network to model the conveyor belt grain dryer using input–output data obtained during an experiment to dry paddy grains. The type 2 simplified ANFIS controller was proposed to control the NARX-based dryer model. The equations were obtained by the MATLAB "nlarx" function [34]. Results showed that the developed NARX model obtained the highest modelling precision compared to other previous studies.

Finally, Lutfy et al. [118] represented the belt dryer model by a sigmoid-based NARX network as it achieves the best modelling performance comparing to other neural networks. An experimental laboratory scale setup was built to compare the results obtained from the NARX model with the experimental data. Using the RMSE criterion, the modelling precision of the optimized sigmoid-based NARX model was evaluated. The proposed sigmoid-based NARX model obtained a 99.74% optimal performance index. Kaveh et al. [119] investigated the thin-layer drying characteristics of turnip slices in a multistage semi-industrial continuous band dryer. An experimental model was set up by varying the drying factors as air temperature, velocity, and belt velocity. They proposed two methods for modelling. In the first method, they used six mathematical models to fit the experimental data. The Midilli et al. [15] model was selected as the best mathematical model. The other models [78,80,84,120,121] showed inferior performance. In the second method, they used an ANN model for the drying process. After proper training of ANN models, it was determined that they were superior to empirical models.

Table 6: Product final moisture content correlations

Author	Correlation	Notes
Bruin et al. [20]	$X_F = X_E\left(T_{airF}, a_W\right) + \left[X_I - X_E\left(T_{airF}, a_W\right)\right] \exp\left[-D_{cons}\left(T_{airF}, X_{airF}, U_{air}, r_C\right) t\right]$	r_C: Characteristic dimension of product particles (m)
Friso [30]	$X_F = X_I + \frac{\overset{\circ}{m}_{air} \cdot c_{air} \cdot (1 + X_I)}{U_{Belt} \cdot r \cdot \rho_{product} \cdot B_I \cdot H_I} \cdot (T_{airE} - T_{airI})\,\eta$	
Midilli et al. [15]	$MR = a \cdot \exp(-K * t^n) + bt$	
Shirinbakhsh et al. [33]	$X_e = b_1 \exp\left[\frac{b_2}{273 + T}\right]\left[\frac{a_w}{1 - a_w}\right]^{b_3}$	

(Continued)

Table 6 (continued)

Author	Correlation	Notes
Montazer-Rahmati et al. [95]	$MR = \frac{X - X_E}{X_i - X_E} = \exp\left(\frac{k_1 \cdot \tau}{1 + k_2 \cdot \tau}\right)$	
	$k_1 = -0.1935\,(0.9289 - U_{air}) + \left(\frac{0.00011\mathrm{Ln}\,(T_{air})}{1.0166 - U_{air}} - \frac{(1.0031 - U_{air}) \cdot \sqrt{T_{air}}}{9250.6938}\right) \cdot T_{air}$	
	$k_2 = -0.1123 \exp\left[\frac{0.0076 T_{air}}{2.8307 - U_{air}} - 2.5877 U_{air}\right] + \frac{T_{air} \cdot \exp\,(-1.8789 U_{air})}{1431.6089}$	
The Page model [98]	$MR = \exp\left(-kt^n\right)$	
The logarithmic model [102]	$MR = a \exp\,(-kt) + c$	
One-term exponential function [103]	$MR = c \exp\,(-kt)$	
Henderson et al. [16]	$\mathrm{MR} = a \exp\,(-kt)$	
Kaveh et al. [119]	$\mathrm{MR} = \frac{8}{\pi^2} \exp\left(-\frac{\pi^2 D_{\mathrm{eff}} \left(\frac{x}{U_b}\right)}{4L^2}\right)$	

Table 7: Heat and mass transfer coefficients correlations

Author	Correlation	Notes
Hosseinizand et al. [22]	$\mathrm{k_m} = 7.586 \times 10^{-4} \cdot \frac{\mathrm{X}}{\mathrm{X} - 0.0622} \cdot \left(1 + \ln \frac{\mathrm{U_{air}}}{0.01389}\right)$	
Friso [29]	$\mathrm{F} \cdot \mathrm{h_m} = \frac{\mathrm{U_{Belt}} \cdot \rho_{\mathrm{product}} \cdot \mathrm{r}}{\mathrm{L_{Belt}} \cdot \Delta \mathrm{T_{mL}}} \cdot \frac{\mathrm{X_I} - \mathrm{X_F}}{(1 + \mathrm{X_I})}$	F: dimension factor
Amer [31]	$\mathrm{h_m} = \frac{\mathrm{k} \times 0.664 \mathrm{Re}^{0.5} \times \mathrm{Pr}^{0.33}}{\mathrm{D_h}}$	
Faggion et al. [44]	$\mathrm{h_m} = \frac{0.135 \mathrm{K_{air}}}{\mathrm{D}} \exp\,(0.0833 \mathrm{Re})$	D: is diameter of twigs
	$\mathrm{k_m} = 10^{-6}\,(\mathrm{T_{air}})^{2.08}\,(\mathrm{U_{air}})^{1.11} + \left(2.95 \times 10^{-5} \mathrm{T_{air}} - 1.73 \times 10^{-3}\right) \exp\left[(0.46 \mathrm{T_{air}} - 61.15)\,\mathrm{U_{air}}\right]$	
Schmalko et al. [45]	$\mathrm{h_m} = 0.205 \left(\frac{\mathrm{K_{air}}}{\mathrm{L}}\right) \mathrm{Re_L^{0.588}}\,\mathrm{Pr}^{1/3}$	For leaves of yerba mate L is leaves thickness
	$\mathrm{h_m} = 0.51 \left(\frac{K_{air}}{d}\right) \mathrm{Re}_d^{0.5}\,\mathrm{Pr}^{0.37}$	For twigs of yerba mate D is Twig diameter
	$k_{mt} = 0.74 \frac{D_g \rho_g}{d} \left(\frac{vd}{\nu}\right)^{0.5} \left(\frac{\nu}{D_g}\right)^{1/3}$	For twigs of yerba mate
	$k_{ml} = 0.0365 \frac{D_g \rho_g}{L} \left(\frac{\nu L}{\nu}\right)^{0.8}$	For leaves of yerba mate
Pang et al. [47]	$h_m = k_m \cdot [c_{air} \cdot \rho_{air}]^{1/3} \cdot \left[\frac{K_{air}}{D}\right]^{2/3}$	Wood chips

(Continued)

Table 7 (continued)

Author	Correlation	Notes
	$k_m = 0.0418 \cdot \left[\frac{U_{air}}{5}\right]^{0.78} \cdot \left[\frac{T_{air}}{314}\right]^{1.17} \cdot \left[\frac{v_{air}}{1.794 \times 10^{-5}}\right]^{-0.45}$	
Koop et al. [50]	$k_m = \frac{1.43\mathrm{X} - 0.14}{(1-\beta)\,\rho_{product}}$	For corn
	$k_m = \left(-3.92 \times 10^{-5} H_R + 5.87 \times 10^{-5}\right) \exp\left[\left(1.24 \times 10^{-2} H_R + 1.79 \times 10^{-2}\right) T_{air}\right]$	Rough rice
	$k_m = 10^{-6}\,(T_{air})^{2.08} \left(\frac{G_{air}}{\rho_{air}}\right)^{1.11} +$ $\left(2.95 \times 10^{-5} T_{air} - 1.73 \times 10^{-3}\right) \exp\left[(0.46 T_{air} - 61.15)\,\frac{G_{air}}{\rho_{air}}\right]$	Mate leaves
	$h_m = \frac{7.14 \times 10^4}{(1-\beta)\,\rho_{product}} \left[\frac{60 G_{air}\,(T_{air} + 273.15)}{P}\right]^{0.6}$	
	$h_m = 671.39 c_{air} G_{air} \left(\frac{2 d_s G_{air}}{\mu_{air}}\right)^{-0.34}$	d_s is equivalent diameter of rough rice
Incropera et al. 2002 [41]	$\mathrm{h_m} = (\mathrm{K/D}) \left(2 + 0.6 \mathrm{Re}^{1/2}\,\mathrm{Pr}^{1/3}\right)$	D: equivalent diameter of a cocoon
Zhang et al. [72]	$k_m = \frac{D_c \left(2 + 0.552 \mathrm{Re}^{\frac{1}{2}} Sc^{\frac{1}{3}}\right)}{L}$	
	$h_m = \begin{cases} 2\frac{k_{\mathrm{eff}}}{L} \frac{0.3387\,\mathrm{Pr}^{\frac{1}{3}}\,\mathrm{Re}^{\frac{1}{2}}}{\left(1 + \left(\frac{0.0468}{\mathrm{Pr}}\right)^{\frac{2}{3}}\right)^{\frac{1}{4}}}, \mathrm{Re} \le 5 \times 10^5 \\ 2\frac{k_{\mathrm{eff}}}{L}\,\mathrm{Pr}^{\frac{1}{3}} \left(0.037 \mathrm{Re}^{\frac{4}{5}} - 871\right), \mathrm{Re} \ge 5 \times 10^5 \end{cases}$	
Montazer-Rahmati et al. [95]	$k_m = \left(386.241 X^{0.5} - 15.614\right)^{-1} \cdot \left(\frac{\exp(0.031 T_{air})}{T_{air}^2}\right) \cdot \exp\left(-\frac{0.33}{U_{air}}\right)$	
Tussolini et al. [110]	$k_1 = 10^{-6}\,(T_{air})^{2.08}\,(U_{air})^{1.11}$	
	$k_2 = \left(\alpha T_g - 1.73 \times 10^{-3}\right) \exp\left[(0.46 T_{air} - 61.15)\,U_{air}\right]$	
	$k_m = k_1 + k_2 \left(\alpha = 2.95 \times 10^{-5}\right)$	

Li et al. [122] designed a control scheme for grain dryers using NARX based PSO-MPC neural network as a prediction tool. They used a mathematical model developed by Li and Cao [122] due to the unavailability of actual dryers, so they can generate data for neural network training to improve the fitting precision. A NARX neural network was proposed to represent the dynamic characteristics of the dryer, and an MPC controller with a PSO optimization algorithm was designed for accurate closed-loop control. Simulations based on a rough mathematical model were conducted due to the unavailability of actual dryers, providing abundant data to train the NARX neural network and test the control scheme's performance. The PSO-MPC scheme demonstrated an error of less than 1% in grain humidity and a control precision of under 0.52% in outlet grain moisture content in simulations under different conditions.

Kaveh et al. [123] used two intelligent methods, ANNs and ANFIS to predict the MR, Energy Utilization (EU), Energy Utilization Ratio (EUR), exergy loss and exergy efficiency of drying process for onion slices in a multi-stage semi-industrial continuous belt. An experimental setup was built and worked for various air temperature, air velocity and belt velocity levels. The results demonstrated that the values of effective moisture diffusivity, colour change, EU, EUR, and exergy loss increase when high levels of air temperature and velocity are combined with a low belt linear motion. While drying time, Specific Energy Consumption (SEC) and exergy efficiency decrease.

Jensen et al. [51] presented a soft-sensor empirical model for controlling the moisture content of mate leaves in a virtual conveyor belt drier. The model was trained on a set of 2000 experimental data points, which were collected from batch drying experiments at various temperature ranges. It was correlated using two PDEs derived from the energy and mass balance for water in the dryer's solid phase. The controller adjusted the tray velocity to compensate for random disturbances in feed moisture content and drying temperature, as verified by successful comparisons between open- and closed-loop responses of discharge moisture content.

Table 8: Modelling results of control methods papers

Author	Dried product	Objectives	Results
Kiranoudis et al. 1994 [108]	Wet raisins	Exploring the dynamics of the drying process and investigating control strategies for optimal management of energy and high-quality product production.	Results indicated that material moisture content at the dryer exit was significantly influenced by both the initial material moisture content and drying air temperature. When the input material moisture content was measured in real-time, a PI-feedback cascade temperature controller effectively maintained desired exit moisture levels. However, introducing a 15-s delay in the measurement sensor resulted in diminished control performance. To enhance control in such scenarios, a simplified lead-lag feedforward controller was incorporated alongside the primary PI-feedback cascade controller.
Dai et al. 2017 [109]	Grains	Investigating effective control strategies for the grain dryer plant and optimizing control performance, including overshoot, accuracy, and anti-disturbance abilities.	Simulation results showed that the genetically optimized fuzzy immune PID controller (GOFIP) outperforms the general PID controller, the fuzzy PID controller, and the fuzzy immune PID controller. The GOFIP controller is able to rapidly reach the desired outlet grain moisture content with no overshoot, better accuracy, and stronger anti-disturbance performance.
Tussolini et al. 2014 [110]	Mate leaves	Evaluating a feedback strategy for controlling the drying process of mate leaves in a thin-layer conveyor-belt dryer.	An existing model for mass transfer coefficient (k_m) underestimated km at lower air velocities (0.075–0.095 m/s). A modified equation was developed for accurate prediction within this range ($R^2 = 0.96$, mean relative error = 11%). The revised model accurately predicted moisture content and temperature of mate leaves across various operating conditions. It was shown that air velocity significantly impacted drying rates of leaves, unlike grains or large particles. A feedback control system successfully regulated moisture content in the dryer's discharge, employing a PID controller and adjusting conveyor belt speed. The authors used closed-loop experiments and were able to show that the outlet moisture content was consistently maintained at desired levels (within 11% of the model) despite variations in feed moisture content (0.5–1.7 dry basis), average drying temperature (70°C–97°C) and set-point (0.1–1.0 dry basis). The control scheme was effective even with non-isothermal conditions and longitudinal temperature gradients within the dryer.

(Continued)

Table 8 (continued)

Author	Dried product	Objectives	Results
Mansor et al. 2011 [111]	Grains	Designing an online self-tuning controller that is robust and adaptive to handle wider parameter variations and disturbances in the grain drying process to achieve improved performance compared to standard QFT controllers, particularly in cases of larger parameter variations.	The online QFT-based self-tuning controller successfully tracked reference moisture content signals and adapted to model parameter changes, improving transient response over time. It effectively attenuated both input and output disturbances, maintaining stability and producing low control signals. The controller outperformed a standard QFT-based controller in handling plant parameter variations, demonstrating superior adaptation and transient response characteristics, especially under large uncertainties (up to 50% variation).
Zanoelo et al. 2008 [112]	Mate leaves	Developing a dynamic model and feedback control strategy for conveyor-belt dryers of mate leaves to maintain the discharge moisture content within acceptable limits by adjusting the belt velocity to compensate for disturbances in operating conditions.	The model and mass transfer coefficient aligned with experimental data from both laboratory and industrial dryers. The proposed PI controller, adjusting conveyor belt velocity, successfully maintains discharge moisture content within the desired range (2.4%–3.4% dry basis) despite disturbances in feed moisture, temperature, and air velocity. Results showed that a derivative action (PID controller) is unnecessary for effective control.
Johansen et al. 2010 [113]	Fish feed	Designing an efficient Model Predictive Control (MPC) to algorithm for the conveyor-belt dryer based on a simplified model and comparing its performance against existing controllers.	A verified and improved model of the conveyor-belt dryer, considering noise and disturbances was developed. The simulation results provided insights into the process dynamics and behaviour. A computationally efficient MPC algorithm specifically designed for the conveyor-belt dryer was developed and compared with basic/existing control configurations. The MPC provides a rapid response while respecting the limitations placed on both product temperature and product temperature rate.
Bakhshipour et al. 2021 [114]	Stevia leaves	Investigating the drying behaviour of stevia leaves using an infrared-assisted continuous-flow hybrid solar dryer to develop mathematical and intelligent models to predict the moisture ratio of the leaves throughout the drying process.	The results of the study showed that the inlet air temperature and infrared (IR) lamp input power had a significant effect on the drying time of stevia leaves. The artificial neural network model was found to be the most accurate in predicting the moisture ratio, with high coefficient of determination (R^2) values of 0.9995 and low root mean squared error (RMSE) and chi-squared error values on the test dataset. Among the mathematical models, the Midilli model was the best-fitted model for most drying conditions.
Lutfy et al. 2010 [115]	Grains	Developing a reliable process model for a conveyor-belt grain dryer using the adaptive neuro-fuzzy inference system (ANFIS) to create a data-driven model that can be used in control system design to improve the efficiency and productivity of the drying process.	The results of the study demonstrate the effectiveness of the ANFIS model compared to other models such as the autoregressive with exogenous input model and the artificial neural network model. By using clustering to identify the structure of the ANFIS network, the model achieves a high level of accuracy. The comparison with other models clearly indicates the superiority of the ANFIS model for grain drying applications.

(Continued)

Table 8 (continued)

Author	Dried product	Objectives	Results
Kaveh et al. 2017 [119]	Turnip slices	Examining the thin-layer drying behaviour of turnip slices in a semi-industrial continuous band dryer to determine the drying kinetics of turnip slices, including the effective moisture diffusivity and activation energy, and to develop and evaluate artificial neural network (ANN) models for predicting moisture ratio (MR) and drying rate.	The results of the study showed that the Midilli et al. model was the most accurate mathematical model for describing the drying kinetics of turnip slices. The effective moisture diffusivity ranged from 8.37×10^{-10} to 4.82×10^{-9} m^2/s, and the activation energy varied from 12.80 to 26.31 kJ/mol. The ANN models, particularly the feed-forward back-propagation network with a 4-10-10-2 structure, Bayesian regulation training algorithm, and threshold functions of tansig-purelin-logsig, provided relatively better predictions for MR and drying rate compared to empirical models. The R^2 values for the prediction of MR and drying rate were 0.9990 and 0.9619, respectively.
Li et al. 2020 [122]	Grains	Improving the accuracy of grain moisture content discharged from grain dryers and enhancing the automation and intelligence of the grain drying process.	Model Predictive Control (MPC) is designed based on the neural network model to achieve precise control of moisture content. The particle swarm optimization algorithm was utilized to optimize the cost function in the MPC. MATLAB simulations are conducted to validate the effectiveness of the proposed control approach. The simulations demonstrate that the neural-network-based model predictive scheme improves the control precision of grain dryers.
Lutfy et al. 2011 [116]	Grains	Using adaptive neuro-fuzzy inference system (ANFIS) as an intelligent control system to address the complex and non-linear nature of the grain drying process.	In their comparative study, the PID-like ANFIS controller was superior over a genetically tuned conventional PID controller in controlling the grain drying process.
Lutfy et al. 2015 [117].	Grains	Developing accurate control-oriented model for a conveyor belt grain dryer using a simplified type 2 adaptive neuro-fuzzy inference system (ANFIS) controller to address the challenges of grain drying (energy consumption, product quality, and environmental effects).	The developed NARX model achieved the best modelling accuracy compared to other previously studies. By comparing the reference step responses of the MPC with the PI-control. The MPC obtained superlative results. It provides a rapid response while respecting the limitations placed on both product temperature and product temperature rate.
Lutfy et al. 2015 [118]	Grains	Developing a highly accurate model for conveyor-belt grain drying system to accurately describe the dynamics of the grain drying process.	The results of the paper showed that the proposed sigmoid-based nonlinear autoregressive with exogenous input (NARX) model achieves the best modelling accuracy compared to previously reported techniques for the same drying process. The model is trained using experimental input-output data collected from the conveyor-belt grain dryer during a real-time experiment. The proposed model achieves a RMSE of 2.776×10^{-17}.
Kaveh et al. 2021 [123]	Onion slices	Applying artificial neural networks (ANNs) and adaptive neuro-fuzzy inference system (ANFIS) to predict the drying properties of onion slices in a multi-stage semi-industrial continuous dryer.	The study demonstrated that the ANN model yielded high prediction accuracies for moisture ratio, energy utilization, energy utilization ratio, exergy loss, and exergy efficiency, with values of 0.9995, 0.9957, 0.9984, 0.9960, and 0.9979, respectively. The ANFIS model achieved prediction accuracies of 0.9998, 0.9972, 0.9991, 0.9962, and 0.9985 for the same parameters.

(Continued)

Table 8 (continued)

Author	Dried product	Objectives	Results
Jensen et al. 2010 [51].	Mate leaves	Developing a soft-sensor model for controlling the moisture content of mate leaves in a virtual conveyor-belt dryer.	The results of the study include the tuning of the parameters of the soft-sensor model based using ~2000 experimental data points of surface temperature and moisture content of mate leaves. The simulations confirmed the reliability of the designed inferential controller in maintaining the desired moisture content of mate leaves despite arbitrary process disturbances. The results demonstrated that the soft sensor is a practical tool and less expensive than the costly online sensors of moisture content theoretical control scheme.

8 Conclusion

In summary, this review paper has presented an in-depth review of the various modeling techniques employed for studying the drying process in a belt drier. The methodologies have been categorized into four distinct groups, including theoretical, CFD, empirical, and controllers. Theoretical and CFD methods have been further sub-grouped into transient and steady-state models, as well as 1-D, 2-D, and 3-D models. The empirical methodology involved the collection of moisture ratio data throughout the drying process, which is subsequently compared to empirical models produced by other researchers. The control method studies have been categorized into two groups: classical control and advanced control studies. The advanced control studies incorporate artificial intelligence-based methodologies, including ANN, ANFIS, and NARX models.

In general, the review has elucidated the methodologies and software employed for each modeling technique, as well as their prospective utility in industrial contexts. The utilization of theoretical and CFD methodologies is advantageous in forecasting the dynamics of complex systems. Conversely, empirical techniques serve the purpose of validating theoretical models and procuring data to facilitate model refinement. Controllers play a crucial role in the optimization of the drying process and the attainment of desired outputs.

Acknowledgement: This work was supported by the American University in Cairo, Egypt.

Funding Statement: This work was supported by the American University in Cairo, Egypt. The authors have no financial or personal relationships to disclose that could be perceived as biasing their work. Agreement Number: CCI-SSE-MENG-10.

Author Contributions: The authors confirm contribution to the paper as follows: study conception and design: Mohamed El-Morsi, Omar Abdelaziz; data collection: Gehad Azmy; analysis and interpretation of results: Gehad Azmy, Mohamed El-Morsi, Omar Abdelaziz; draft manuscript preparation: Gehad Azmy, Mohamed El-Morsi, Omar Abdelaziz. All authors reviewed the results and approved the final version of the manuscript.

Availability of Data and Materials: Not applicable.

Ethics Approval: Not applicable.

Conflicts of Interest: The authors declare no conflicts of interest to report regarding the present study.

References

1. Esper A, Mühlbauer W. Solar drying—an effective means of food preservation. Renew Energy. 1998;15(1):95–100. doi:10.1016/S0960-1481(98)00143-8.
2. Fellows PJ. Food processing technology. 3rd ed. Cambridge: Woodhead Publishing Limited; 2007.
3. Omolola AO, Jideani AIO, Kapila PF. Quality properties of fruits as affected by drying operation. Crit Rev Food Sci Nutr. 2017 Jan;57(1):95–108. doi:10.1080/10408398.2013.859563.
4. Qiu J. Mild conductive drying of foods. Wageningen; 2019. doi:10.18174/469413.
5. EL-Mesery HS. Improving the thermal efficiency and energy consumption of convective dryer using various energy sources for tomato drying. Alex Eng J. 2022 Dec;61(12):10245–61. doi:10.1016/j.aej.2022.03.076.
6. Ziegler T, Jubaer H, Teodorov T. Bottlenecks in continuous hops drying with conveyor-belt dryer. Dry Technol. 2022;40(13):2598–616. doi:10.1080/07373937.2021.1950168.
7. Pasban A, Sadrnia H, Mohebbi M, Shahidi SA. Spectral method for simulating 3D heat and mass transfer during drying of apple slices. J Food Eng. 2017;212(3):201–12. doi:10.1016/j.jfoodeng.2017.05.013.
8. Qiu J, Acharya P, Jacobs DM, Boom RM, Schutyser MAI. A systematic analysis on tomato powder quality prepared by four conductive drying technologies. Innov Food Sci Emerg Technol. 2019;54:103–12. doi:10.1016/j.ifset.2019.03.013.
9. Tayel SA, Alkatary HS, Nagy KS, Younes OS. Dehydration of onion slices in IR-refractance window drying system. MISR J Agricul Eng. 2012;29(1):409–28.
10. Mahanti NK, Chakraborty SK, Sudhakar A, Verma DK, Shankar S, Thakur M, et al. Refractance WindowTM-drying vs. other drying methods and effect of different process parameters on quality of foods: a comprehensive review of trends and technological developments. Future Foods. 2021 Jun 01;3(1):100024. doi:10.1016/j.fufo.2021.100024.
11. Genesis. Genesis screen printing conveyor dryer–6ft. Available from: https://screenprintingsupply.com/products/genesis-screen-printing-conveyor-dryer-6ft. [Accessed 2024].
12. The Lens. Available from: https://www.lens.org/. [Accessed 2023].
13. ScienceDirect. Available from: https://www.sciencedirect.com/. [Accessed 2023].
14. Web of Science. Available from: https://www.webofscience.com/. [Accessed 2023].
15. Midilli A, Kucuk H, Yapar Z. A new model for single-layer drying. Dry Technol. 2002;20(7):1503–13. doi:10.1081/DRT-120005864.
16. Henderson SM, Pabis S. Grain drying theory (I) temperature effect on drying coefficient. J Agric Eng Res. 1961;6:169–74.
17. Kaya A, Aydin O, Demirtaş C. Drying kinetics of red delicious apple. Biosyst Eng. 2007 Apr;96(4):517–24. doi:10.1016/j.biosystemseng.2006.12.009.
18. Lewis WK. The rate of drying of solid materials. J Ind Eng Chem. 1921 May;13(5):427–32. doi:10.1021/ie50137a021.
19. Kiranoudis CT, Maroulis ZB, Marinos-Kouris D. Modelling and design of conveyor belt dryers. J Food Eng. 1994;23(3):375–96.
20. Bruin S, Luyben KCAM. Drying of food materials: a review of recent developments. Adv Dry. 1980;1.
21. Kiranoudis CT, Maroutis ZB, Marinos-Kouris D. Design and operation of convective industrial dryers. AIChE J. 1996;42(11):3030–40.
22. Hosseinizand H, Lim CJ, Webb E, Sokhansanj S. Economic analysis of drying microalgae Chlorella in a conveyor belt dryer with recycled heat from a power plant. Appl Therm Eng. 2017;124:525–32. doi:10.1016/j.applthermaleng.2017.06.047.

23. Sebastian P, Nadeau JP, Puiggali JR. Designing dryers using heat and mass exchange networks: an application to conveyor belt dryers. Chem Eng Res Des. 1996;74(8):934–43. doi:10.1205/026387696523102.
24. de Souza Barrozo MA, Murata VV, Assis AJ, Freire JT. Modeling of drying in moving bed. Dry Technol. 2006;24(3):269–79. doi:10.1080/07373930600564530.
25. Petzold LR. DASSL. A differential/algebraic system solver. In: Technical report. Washington, DC, USA: USDOE; 1982 Sep 1.
26. Holowaty SA, Schmalko ME, Schvezov CE. Modeling of a double pass belt conveyer dryer of yerba mate. Dry Technol. 2022;40(5):938–47. doi:10.1080/07373937.2020.1839488.
27. Vaxelaire J, Puiggali JR. Analysis of the drying of residual sludge: from the experiment to the simulation of a belt dryer. Dry Technol. 2002;20(4–5):989–1008. doi:10.1081/DRT-120003773.
28. Xue Q, Miao K, Yu Y, Li Z. A novel method for vacuum belt drying process optimization of licorice. J Food Eng. 2022 Sep;328(20):111075. doi:10.1016/j.jfoodeng.2022.111075.
29. Friso D. Conveyor-belt dryers with tangential flow for food drying: mathematical modeling and design guidelines for final moisture content higher than the critical value. Inventions. 2020;5(2):1–15. doi:10.3390/inventions5020022.
30. Friso D. Conveyor-belt dryers with tangential flow for food drying: development of drying odes useful to design and process adjustment. Inventions. 2021;6(1):1–12. doi:10.3390/inventions6010006.
31. Eng MJA, Amer BMA. Process Engineering Mathematical Modeling of temperature and heat profiles in pilot Refractance Window drying system; 2011. Available from: https://doi.org/10.21608/mjae.2011.102614. [Accessed 2024].
32. Nindo CI, Tang J, Powers JR, Bolland K. Energy consumption during Refractance Window® evaporation of selected berry juices. Int J Energy Res. 2004 Oct;28(12):1089–100. doi:10.1002/er.1017.
33. Shirinbakhsh M, Amidpour M. Design and optimization of solar-assisted conveyer-belt dryer for biomass. Energy Equipment Syst. 2017;5(2):1–10.
34. The MathWorks Inc. Statistics and machine learning toolbox. Natick, MA, USA: The Math Works Inc.; 2022.
35. Perry RH, Green DW. Perry's chemical engineer's. 8th ed. New York: McGraw-Hill; 1999.
36. Maroulis ZB, Saravacos GD. Food process design. New York, USA: Marcel Dekker; 2003.
37. Canabarro NI, Mazutti MA, do Carmo Ferreira M. Drying of olive (*Olea europaea* L.) leaves on a conveyor belt for supercritical extraction of bioactive compounds: mathematical modeling of drying/extraction operations and analysis of extracts. Ind Crops Prod. 2019 Sep;136(2):140–51. doi:10.1016/j.indcrop.2019.05.004.
38. Mirzahoseinkashani E, Kasiri N. Mathematical modeling of a cross flow conveyor belt dryer. Sci Iran. 2008;15(4):494–501.
39. Rossi SJ. ìPsychrometryî. Jo, o Pessoa: FUNAPE; 1987 (In Portuguese).
40. Jumah RY, Mujumdar AS, Raghavan GSV. A mathematical model for constant and intermittent batch drying of grains in a novel rotating jet spouted bed. Dry Technol. 1996;14(3–4):765–802.
41. Incropera FP, DeWitt DP. Fundamentals of heat and mass transfer. 7th ed. New York: John Wiley & Sons; 2002.
42. Inc. Wolfram Research. Mathematica. 14. Available from: https://www.wolfram.com/mathematica/. [Accessed 2024].
43. Salemović DR, Dedić AD, Ćuprić NL. A mathematical model and simulation of the drying process of thin layers of potatoes in a conveyor-belt dryer. Therm Sci. 2015;19(3):1107–18. doi:10.2298/TSCI130920020S.
44. Faggion H, Tussolini L, Freire FB, Freire JT, Zanoelo EF. Mechanisms of heat and mass transfer during drying of mate (*Ilex paraguariensis*) twigs. Dry Technol. 2016;34(4):474–82. doi:10.1080/07373937.2015.1060498.

45. Schmalko ME, Peralta JM, Alzamora SM. Modeling the drying of a deep bed of ilex paraguariensis in an industrial belt conveyor dryer. Dry Technol. 2007 Dec;25(12):1967–75. doi:10.1080/07373930701727317.
46. Burmester K, Eggers R. Heat and mass transfer during drying of liquid pasty plant extract by vacuum belt drying. Dry Technol. 2012 Jan;30(1):29–36. doi:10.1080/07373937.2011.615034.
47. Pang S, Xu Q. Drying of woody biomass for bioenergy using packed moving bed dryer: mathematical modeling and optimization. Dry Technol. 2010 May;28(5):702–9. doi:10.1080/07373931003799251.
48. Neto AN. Dryer modeling and optimization. Texas: Faculty of Texas Tech University; 1997.
49. Ostrikov AN, Ospanov AA, Shevtsov AA, Muslimov NZ, Timurbekova AK, Jumabekova GB. Mathematical model of high-temperature tubeshaped pasta drying in a conveyer belt drier. Int J Food Eng. 2021;17(3):209–15. doi:10.1515/ijfe-2020-0101.
50. Koop L, Tussolini L, Pedersen Voll FA, Zanoelo EF. A dynamic two-dimensional model for deep-bed drying of mate leaves (*Ilex paraguariensis*) in a single-pass/single-zone conveyor-belt dryer. Dry Technol. 2015;33(2):185–93. doi:10.1080/07373937.2014.943236.
51. Jensen S, da Cruz Meleiro LA, Zanoelo É.F. Soft-sensor model design for control of a virtual conveyor-belt dryer of mate leaves (*Ilex paraguariensis*). Biosyst Eng. 2011;108(1):75–85. doi:10.1016/j.biosystemseng.2010.10.012.
52. Sorokovaya NN, Snezhkin YF, Shapar' RA, Sorokovoi RY. Mathematical simulation and optimization of the continuous drying of thermolabile materials. J Eng Phys Thermophys. 2019 Sep;92(5):1180–90. doi:10.1007/s10891-019-02032-3.
53. Lima AGB, Mata SF. Study of the silkworm cocoon drying kinetic; 1996.
54. Khankari KK, Patankar SV. Performance analysis of a double-deck conveyor dryer—a computational approach. Dry Technol. 1999;17(10):2055–67. doi:10.1080/07373939908917672.
55. Böhner M, Barfuss I, Heindl A, Müller J. Improving the airflow distribution in a multi-belt conveyor dryer for spice plants by modifications based on computational fluid dynamics. Biosyst Eng. 2013 Jul;115(3):339–45. doi:10.1016/j.biosystemseng.2013.03.012.
56. ANSYS, Inc. ANSYS fluent–CFD software. ANSYS, Inc.; 2023. Available from: https://www.ansys.com/products/fluids/ansys-fluent. [Accessed 2024].
57. Zhang Q, Huang M, Wang J, Zhang P, Chen B, Shi Z, et al. Investigation on airflow distribution under different feed thickness combined CFD modeling and experimental verification. Dry Technol. 2020;39(3):306–23. doi:10.1080/07373937.2020.1777561.
58. Mondal S, Dutta S, Pande P, Naik-Nimbalkar V. Intensify staple fibre drying by optimizing air distribution in multistage convective dryer using CFD. Chem Eng Process-Process Intensif. 2022 Mar;173(1):108807. doi:10.1016/j.cep.2022.108807.
59. Chang J, Qi T-T, Liu X-D. Numerical simulation and optimization of a multilayer belt dryer for granular food materials. Pittsburgh, PA, USA: American Society of Agricultural and Biological Engineers (ASABE); 2010. doi:10.13031/2013.29703.
60. Alamia A, Ström H, Thunman H. Design of an integrated dryer and conveyor belt for woody biofuels. Biomass Bioenergy. 2015;77(Suppl. 1):92–109. doi:10.1016/j.biombioe.2015.03.022.
61. Aspen Plus V8.2. Aspen Technology, Inc.
62. Selimefendigil F, Coban SO, Öztop HF. Numerical analysis of heat and mass transfer of a moving porous moist object in a two dimensional channel. Int Commun Heat Mass Transf. 2021 Feb;121:105093. doi:10.1016/j.icheatmasstransfer.2020.105093.
63. COMSOL Multiphysics(R). V. 6.3. Stockholm. Sweden: COMSOL, AB. Available from: https://cn.comsol.com/. [Accessed 2024].
64. Zhang H, Deng S. Numerical simulation of moisture-heat coupling in belt dryer and structure optimization. Appl Therm Eng. 2017 Dec;127(6):292–301. doi:10.1016/j.applthermaleng.2017.08.071.

65. Thorpe GR. The application of computational fluid dynamics codes to simulate heat and moisture transfer in stored grains. J Stored Prod Res. 2008;44(1):21–31. doi:10.1016/j.jspr.2007.07.001.
66. Hunter A. On the heat of sorption of australian paddy rice. J Agric Eng Res. 1989 Sep–Dec;44(2):237–9. doi:10.1016/S0021-8634(89)80085-X.
67. Zhang H, Pang B, Kang S, Fu J, Tang P, Chang J, et al. The influence of feedstock stacking shape on the drying performance of conveyor belt dryer. Heat Mass Trans/Waerme-und Stoffuebertragung. 2022;58(1):157–70. doi:10.1007/s00231-021-03098-7.
68. Çoban SÖ, Selimefendigil F, Öztop HF. 3D numerical study of heat and mass transfer of moving porous moist objects. Therm Sci Eng Progress. 2021 Aug;24(4):100939. doi:10.1016/j.tsep.2021.100939.
69. Akpinar EK, Dincer I. Application of moisture transfer models to solids drying. Proc Inst Mech Eng Part A: J Power Energy. May 2005;219(3):235–44. doi:10.1243/095765005X7538.
70. Shen L, Zhu Y, Liu C, Wang L, Liu H, Kamruzzaman M, et al. Modelling of moving drying process and analysis of drying characteristics for germinated brown rice under continuous microwave drying. Biosyst Eng. 2020 Jul;195(1):64–88. doi:10.1016/j.biosystemseng.2020.05.002.
71. Zhou J, Yang X, Chu Y, Li X, Yuan J. A novel algorithm approach for rapid simulated microwave heating of food moving on a conveyor belt. J Food Eng. 2020 Oct;282(4):110029. doi:10.1016/j.jfoodeng.2020.110029.
72. Zhang Y, Gao M, Gao F, Yang H, Liu Y, Zheng X. Puffing characteristics of berry slice under continuous microwave puffing conditions. J Food Process Preserv. 2022 Oct;46(10). doi:10.1111/jfpp.16838.
73. Zhang P, Wu P, Zhang Q, Shi Z, Wei M, Jaberi-Douraki M. Optimization of feed thickness on distribution of airflow velocity in belt dryer using computational fluid dynamics. Energy Procedia; 2017;142:1595–602. doi:10.1016/j.egypro.2017.12.536.
74. Zhang P, Huwag MF, Sutar PP, Wang J, Zhang Q, Zhang J, et al. Effect of fan frequency on the air flow distribution and moisture content in aquatic feed belt dryer with CFD simulation and experimental verification. Appl Eng Agric. 2022;38(5):729–39. doi:10.13031/aea.14720.
75. Ortiz-Jerez MJ, Gulati T, Datta AK, Ochoa-Martínez CI. Quantitative understanding of refractance window™ drying. Food Bioprod Process. 2015;95(7):237–53. doi:10.1016/j.fbp.2015.05.010.
76. Zhang P, Mu Y, Shi Z, Zhang Q, Wei M, Jaberi-Douraki M. Computational fluid dynamic analysis of airflow in belt dryer: effects of conveyor position on airflow distribution. Energy Proc. 2017;142(1):1367–74. doi:10.1016/j.egypro.2017.12.521.
77. Soodmand-Moghaddam S, Sharifi M, Zareiforoush H, Mobli H. Mathematical modelling of lemon verbena leaves drying in a continuous flow dryer equipped with a solar pre-heating system. Qualit Assur Saf Crops Foods. 2020;12(1):57–66. doi:10.15586/QAS2019.658.
78. Page GE. Factors influencing the maximum rates of air drying shelled corn in thin layers. West Lafayette, IN, USA: Purdue University; 1949. Available from: https://docs.lib.purdue.edu/dissertations/AAI1300089/. [Accessed 2024].
79. White GM, Bridges TC, Loewer OJ, Ross IJ. Thin-layer drying model for soybeans. Trans ASAE. 1981;24(6):1643–6. doi:10.13031/2013.34506.
80. Wang GY, Singh RP. Single layer drying equation for rough rice. Agricul Food Sci. 1978.
81. Badaoui O, Hanini S, Djebli A, Haddad B, Benhamou A. Experimental and modelling study of tomato pomace waste drying in a new solar greenhouse: evaluation of new drying models. Renew Energy. 2019 Apr;133(10):144–55. doi:10.1016/j.renene.2018.10.020.
82. Vijayan S, Arjunan TV, Kumar A. Mathematical modeling and performance analysis of thin layer drying of bitter gourd in sensible storage based indirect solar dryer. Innovat Food Sci Emerg Technol. 2016 Aug;36(3):59–67. doi:10.1016/j.ifset.2016.05.014.
83. Guan Z, Wang X, Li M, Jiang X. Mathematical modeling on hot air drying of thin layer fresh tilapia fillets. Pol J Food Nutr Sci. 2013 Mar;63(1):25–34. doi:10.2478/v10222-012-0065-5.

84. Torki-Harchegani M, Ghanbarian D, Ghasemi Pirbalouti A, Sadeghi M. Dehydration behaviour, mathematical modelling, energy efficiency and essential oil yield of peppermint leaves undergoing microwave and hot air treatments. Renew Sustain Energ Rev. 2016 May;58(22):407–18. doi:10.1016/j.rser.2015.12.078.
85. IBM Corp. IBM SPSS. IBM: 11.5.1.
86. Soodmand-Moghaddam S, Sharifi M, Zareiforoush H. Investigation of fuel consumption and essential oil content in drying process of lemon verbena leaves using a continuous flow dryer equipped with a solar pre-heating system. J Clean Prod. 2019 Oct;233:1133–45. doi:10.1016/j.jclepro.2019.06.083.
87. Chayjan RA, Kaveh M, Khayati S. Modeling some thermal and physical characteristics of terebinth fruit under semi industrial continuous drying. J Food Meas Charact. 2017 Mar;11(1):12–23. doi:10.1007/s11694-016-9366-4.
88. Shi J, Pan Z, McHugh TH, Wood D, Zhu Y, Avena-Bustillos RJ, et al. Effect of berry size and sodium hydroxide pretreatment on the drying characteristics of blueberries under infrared radiation heating. J Food Sci. 2008 Aug;73(6):109. doi:10.1111/j.1750-3841.2008.00816.x.
89. Kaveh M, Chayjan RA. Modeling drying characteristics of terebinth fruit under infrared fluidized bed condition. Cercet Agronomice Moldova. 2015 May;47(4):5–21. doi:10.1515/cerce-2015-0001.
90. Hyams DG. CurveExpert software. online: Daniel G. Hyams. Ed. Available from: https://www.curveexpert.net/. [Accessed 2024].
91. Jafarifar M, Chayjan RA, Dibagar N, Alaei B. Modelling some engineering properties of walnut kernel undergoing different drying methods with microwave pre-treatment. Qual Assur Saf Crops Foods. 2017;9(4):463–78. doi:10.3920/QAS2017.1071.
92. Wang HC, Zhang M, Adhikari B. Drying of shiitake mushroom by combining freeze-drying and mid-infrared radiation. Food Bioprod Process. 2015 Apr;94(2):507–17. doi:10.1016/j.fbp.2014.07.008.
93. Janjai S, Mahayothee B, Lambert N, Bala BK, Precoppe M, Nagle M, et al. Diffusivity, shrinkage and simulated drying of litchi fruit (*Litchi Chinensis Sonn*.). J Food Eng. 2010 Jan;96(2):214–21. doi:10.1016/j.jfoodeng.2009.07.015.
94. Dash KK, Gope S, Sethi A, Doloi M. Study on thin layer drying characteristics star fruit slices. Int J Agricul Food Sci Technol. 2013;4(7):679–86.
95. Montazer-Rahmati MM, Amini-Horri B. From laboratory experiments to design of a conveyor-belt dryer via mathematical modeling. Dry Technol. 2005 Dec;23(12):2389–420. doi:10.1080/07373930500340460.
96. Benjamin E, Grabe DF. Develpment of oven and Karl Fischer Techniques for moisture testing of grass seeds. J Seed Technol. 1988;12(1):76–89.
97. Microsoft Corporation. Table curve software in microsoft excel. Microsoft Corporation.
98. Yang MJ, Liu B, Yang ZR, Ding ZY, Yang L, Xie SY, et al. Development and experimental study of Infrared belt dryer for rapeseed. INMATEH Agricul Eng. 2017;53(3):71–80.
99. Doymaz İ, Karasu S, Baslar M. Effects of infrared heating on drying kinetics, antioxidant activity, phenolic content, and color of jujube fruit. J Food Meas Charact. 2016 Jun;10(2):283–91. doi:10.1007/s11694-016-9305-4.
100. Ostrikov A, Ospanov A, Shevtsov A, Vasilenko V, Timurbekova A. An empirical-mathematical modelling approach to explore the drying kinetics of cereals under variable heat supply using the stitched method. Acta Agric Scand B Soil Plant Sci. 2021;71(9):762–71. doi:10.1080/09064710.2021.1947360.
101. Ogunnaike F, Olalusi AP. Modelling kinetics of extruded fish feeds in a continuous belt dryer. Turk J Agricul Eng Res. 2021 Dec;2(2):289–97. doi:10.46592/turkager.
102. Liu X, Qiu Z, Wang L, Cheng Y, Qu H, Chen Y. Mathematical modeling for thin layer vacuum belt drying of Panax notoginseng extract. Energy Convers Manag. 2009 Apr;50(4):928–32. doi:10.1016/j.enconman.2008.12.032.
103. Fumagalli F, Freire JT. Analysis of the drying kinetics of *Brachiaria brizantha* (Hochst. stapf) grass seeds at different drying modes. Dry Technol. 2007;25(9):1437–44. doi:10.1080/07373930701536734.

104. Brooker DB, Bakker-Arkema FW, Carl W. Drying Cereal Grains. 2nd ed. Westport, CT, USA: AVI Publishing Company; 1974.
105. Xu S, Kerr WL. Modeling moisture loss during vacuum belt drying of low-fat tortilla chips. Dry Technol. 2012 Oct;30(13):1422–31. doi:10.1080/07373937.2012.685999.
106. Jafari H, Kalantari D, Azadbakht M. Semi-industrial continuous band microwave dryer for energy and exergy analyses, mathematical modeling of paddy drying and it's qualitative study. Energy. 2017;138(3):1016–29. doi:10.1016/j.energy.2017.07.111.
107. Zareiforoush H, Bakhshipour A, Bagheri I. Performance evaluation and optimization of a solar-assisted multi-belt conveyor dryer based on response surface methodology. J Renew Energy Environ. 2022 Jan;9(1):78–92.
108. Kiranoudis CT, Maroulis ZB, Marinos-Kouris D. Dynamic simulation and control of conveyor-belt dryers. Dry Technol. 1994 Jan;12(7):1575–603. doi:10.1080/07373939408962188.
109. Dai A, Zhou X, Liu X. Design and simulation of a genetically optimized fuzzy immune PID controller for a novel grain dryer. IEEE Access. 2017 Jul;5:14981–90. doi:10.1109/ACCESS.2017.2733760.
110. Tussolini L, de Oliveira JS, Freire FB, Freire JT, Zanoelo EF. Thin-layer drying of mate leaves (*Ilex paraguariensis*) in a Conveyor-belt dryer: a semi-automatic control strategy based on a dynamic model. Dry Technol. 2014;32(12):1457–65. doi:10.1080/07373937.2014.900504.
111. Mansor H, Noor SBM, Ahmad RKR, Taip FS. Online quantitative feedback theory (QFT)-based self-tuning controller for grain drying process. Sci Res Essays. 2011 Dec;6(31):6520–34. doi:10.5897/SRE11.1337.
112. Zanoelo EF, Abitante A, Meleiro LAC. Dynamic modeling and feedback control for conveyors-belt dryers of mate leaves. J Food Eng. 2008 Feb;84(3):458–68. doi:10.1016/j.jfoodeng.2007.06.008.
113. Johansen Van Delft T. Modeling and model predictive control of a conveyor-belt dryer applied to the drying of fish feed. Trondheim, Norway: NTNU–Norwegian University of Science and Technology. Available from: http://hdl.handle.net/11250/260805. [Accessed 2024].
114. Bakhshipour A, Zareiforoush H, Bagheri I. Mathematical and intelligent modeling of stevia (*Stevia Rebaudiana*) leaves drying in an infrared-assisted continuous hybrid solar dryer. Food Sci Nutr. 2021 Jan;9(1):532–43. doi:10.1002/fsn3.2022.
115. Lutfy OF, Noor SBM, Marhaban MH, Abbas KA, Mansor H. Neuro-fuzzy modeling of a conveyor-belt grain dryer. J Food Agric Environ. 2010;8(4):128–34.
116. Lutfy OF, Mohd Noor SB, Marhaban MH, Abbas KA. Non-linear modelling and control of a conveyor-belt grain dryer utilizing neuro-fuzzy systems. Proc Inst Mech Eng Part I: J Syst Control Eng. 2011 Aug;225(5):611–22. doi:10.1177/2041304110394559.
117. Lutfy OF, Selamat H, Mohd Noor SB. Intelligent modeling and control of a conveyor belt grain dryer using a simplified type 2 neuro-fuzzy controller. Dry Technol. 2015 Jul;33(10):1210–22. doi:10.1080/07373937.2015.1021007.
118. Lutfy OF, Selamat H, Noor SBM. Modelling of a conveyor-belt grain dryer utilizing a sigmoid network. In: 10th Asian Control Conference (ASCC); 2015 Sep; Kota Kinabalu, Malaysia: IEEE. doi:10.1080/07373937.2015.1021007.
119. Kaveh M, Amiri Chayjan R. Modeling thin-layer drying of turnip slices under semi-industrial continuous band dryer. J Food Process Preserv. 2017 Apr;41(2):e12778. doi:10.1111/jfpp.12778.
120. Demir V, Gunhan T, Yagcioglu AK. Mathematical modelling of convection drying of green table olives. Biosyst Eng. 2007 Sep;98(1):47–53. doi:10.1016/j.biosystemseng.2007.06.011.
121. Chayjan RA, Kaveh M. Physical parameters and kinetic modeling of fix and fluid bed drying of terebinth seeds. J Food Process Preserv. 2014;38(3):1307–20. doi:10.1111/jfpp.12092.

122. Li H, Chen S. A neural-network-based model predictive control scheme for grain dryers. Dry Technol. 2020 Jun;38(8):1079–91. doi:10.1080/07373937.2019.1611598.

123. Kaveh M, Chayjan RA, Golpour I, Poncet S, Seirafi F, Khezri B. Evaluation of exergy performance and onion drying properties in a multi-stage semi-industrial continuous dryer: artificial neural networks (ANNs) and ANFIS models. Food Bioprod Process. 2021 May;127(13):58–76. doi:10.1016/j.fbp.2021.02.010.